AJAE

Open Access

Vol. 14, No. 2, pp. 85-104, June 2020
doi: https://doi.org/10.5572/ajae.2020.14.2.85
ISSN (Online) 2287-1160, ISSN (Print) 1976-6912

Review Article

# Conducting Polymer Nanofibers based Sensors for Organic and Inorganic Gaseous Compounds

**Ali Mirzaei[1),†], Vanish Kumar[2),†], Maryam Bonyani[3)], Sanjit Manohar Majhi[4),5)], Jae Hoon Bang[6)], Jin-Young Kim[5)], Hyoun Woo Kim[4),6),*], Sang Sub Kim[5),*], Ki-Hyun Kim[7),*]**

[1)]Department of Materials Science and Engineering, Shiraz University of Technology, Shiraz 71557-13876, Iran
[2)]National Agri-Food Biotechnology Institute (NABI), S.A.S. Nagar, Punjab, 140306, India
[3)]Department of Materials Science and Engineering, Shiraz University, Shiraz 71454, Iran
[4)]The Research Institute of Industrial Science, Hanyang University, Seoul 04763, Republic of Korea
[5)]Department of Materials Science and Engineering, Inha University, Incheon 22212, Republic of Korea
[6)]Division of Materials Science and Engineering, Hanyang University, Seoul 04763, Republic of Korea
[7)] Department of Civil and Environmental Engineering, Hanyang University, 222 Wangsimni-ro, Seoul, 04763, Republic of Korea

[†]These two authors contributed equally to this work as co-first authors.

***Corresponding author.**
E-mail: hyounwoo@hanyang.ac.kr
E-mail: sangsub@inha.ac.kr
E-mail: kkim61@hanyang.ac.kr

**Received:** 27 February 2020
**Revised:** 12 March 2020
**Accepted:** 27 March 2020

**ABSTRACT** Resistive-based gas sensors built through the combination of semiconducting metal oxides and conducting polymers (CPs) are widely used for the detection of diverse gaseous components. In light of the great potential of each of these components, electrospun CPs produced by a facile electrospinning method can offer unique opportunities for the fabrication of sensitive gas sensors for diverse gaseous compounds due to their large surface area and favorable nanomorphologies. This review focuses on the progress achieved in gas sensing technology based on electrospun CPs. We offer numerous examples of CPs as gas sensors and discuss the parameters affecting their sensitivity, selectivity, and sensing mechanism. This review paper is expected to offer useful insights into potential applications of CPs as gas sensing systems.

**KEY WORDS** Conductive polymer, Nanofibers, Electrospinning, Gas sensor, Sensing mechanism

## 1. INTRODUCTION

To eliminate the ongoing environmental problems affecting our livelihood activities, gas sensors are regarded as effective tools to monitor and quantify air pollutants in ambient air and industrial effluetns in various application fields such as medical diagnosis, analytical laboratories, military applications, mines and indoor environments (Mirzaei *et al.*, 2016; Korotcenkov, 2007; Yamazoe, 2005; Azad *et al.*, 1992). The successful commercialization of gas sensors was possible after the pioneering works on metal oxide semiconductor (MOS)-based chemiresistive gas sensors in the 1960s (Seiyama *et al.*, 1962; Taguchi, 1962). Today, MO-based chemiresistive gas sensors are highly popular due to their various advantages such as high sensitivity, simple fabrication, high stability, small size (portability), and low cost (Mirzaei *et al.*, 2016; Wang *et al.*, 2010; Korotcenkov, 2007; Yamazoe, 2005; Azad *et al.*, 1992). In MO-based resistive sensors, the types and concentrations of gases affect the electrical resistance of the sensor (Lin *et al.*, 2017). Response to a target gas, selectivity, stability, sensing temperature, and response time/recovery time are very important features of a gas sensor (Baharuddin *et al.*, 2019; Lin *et al.*, 2017; Miller *et al.*, 2014;

Wang *et al.*, 2010). Among them, sensing temperature is a key parameter that controls the overall consumption of power for the operation of gas sensors. Unfortunately, as the sensing temperatures of most of resistive-based gas sensors are high (up to 450°C), it can increase in power consumption while shortening the sensor lifespan (Miller *et al.*, 2014).

Conducting polymers (CPs) can be used for sensing studies to deal with the high sensing temperature of MO-based gas sensors (Patil *et al.*, 2012). These structures are the organic materials with intrinsic electrical conductivity (Gerard *et al.*, 2002). In general, the presence of π-electron backbone is the main reason for their extraordinary electrical properties, low ionization potential, low energy optical transitions, and high electron affinity. These unique characteristics of CPs have tremendous potential toward sensing applications for diverse gases. CPs have the ability to achieve good sensing characteristics at low or room temperature and to tune their physical and chemical properties to improve the sensing properties (Fratoddi *et al.*, 2015). Furthermore, they have other advantages such as low-temperature synthesis, high flexibility, the possibility of large-scale synthesis, and low costs (Janata and Josowicz, 2003). In particular, CPs can be easily synthesized and their molecular chain structure can be easily improved by controlling synthesis parameters (Talwar *et al.*, 2014; Jung *et al.*, 2008; Bartlett and Ling-Chung, 1989). These advantageous attributes have spurred interest in further study of CP-based chemiresistive gas sensors. Accordingly, some CPs such as polyaniline (PANI), polythiophene, polypyrrole (PPy) and their derivatives have been studied as gas sensing materials since the 1980s (Nylander *et al.*, 1983). The sensing performance of a gas sensor relies on its morphology, microstructure and size (Shimizu and Egashira, 1999; Yamazoe, 1991). Hence, synthesizing nano-scale based CPs for sensing applications would be beneficial for sensing studies. Among different nanostructures, one-dimensional (1D) nanomaterials, such as nanowires, nanorods, nanotubes and nanofibers (NFs), are considered to be very interesting for sensing applications (Arafat *et al.*, 2012). The advantages of 1D nanomaterials are large surface area, high charge carrier collection and transport in the axial orientation and the possibility of surface modification (Chinnappan *et al.*, 2017).

Among these 1D nanostructures, the electrospun NFs offer high surface area, which is suitable for the adsorption of target gases and allows rapid diffusion of gases species, thus increasing the sensor response (Chinnappan *et al.*, 2017). Furthermore, since the diameters of electrospun CP NFs are in the nanoscale range, they offer many interesting properties such as excellent flexibility in surface functionality and better mechanical properties relative to their micro scale counterparts (Yanılmaz and Sarac, 2014). In addition to gas sensing applications, CPs NFs are promising candidates for many other practical applications (Kelly *et al.*, 2013; Moon *et al.*, 2013; Zhao *et al.*, 2013; Sowmiya *et al.*, 2012; Bejbouji *et al.*, 2010; Dhand *et al.*, 2010; Huang *et al.*, 2003). However, in this survey, we only focused on the gas sensing applications of electrospun CPs. Several reviews have already been published on CPs and their derivatives for gas sensing applications (Park *et al.*, 2017; Pandey, 2016; Hangarter *et al.*, 2013; Bai and Shi, 2007; Shirakawa *et al.*, 1977). However, to the best of our knowledge, CPs synthesized by electrospinning method such as NF-based CPs have not been reviewed yet. Herein, we have focused on the CPs-based chemoresistive gas sensors. The major focus of this review is to cover the materials developed through electrospinning processes. However, in a few cases, we also covered CP-based materials prepared by other methods for comparison purpose. In this review, we provided a general introduction about CPs (Section 2) and electrospinning process (Section 3). In section 4, we have discussed the CPs-based gas sensors and their mechanism of gas sensing. In the last section, we drew a conclusion of the present work with future suggestions.

## 2. CONDUCTIVE POLYMERS (CPS)

In the late 1970s, it was demonstrated that polymers having π-conjugated chains have excellent conductivity in partially reduced or oxidized states (Chiang *et al.*, 1978; Shirakawa *et al.*, 1977). In 2000, CP research gained more attention after the Nobel Prize in Chemistry was given for work on CPs. CPs (or simply conjugated polymers) are a special class of polymers containing a $sp^2$ structure with alternating π-bonds that allow delocalized transport of charge carriers (Heeger, 2001). They have the advantages of excellent electronic properties, easy synthesis procedure, tunable properties, flexibility, and environmental stability. As shown in Fig. 1, the most important CPs include polyaniline (PANI), poly(3, 4-ethylenedioxythiophene) (PEDOT), polyacetylene

(PA), polythiophene (PTh), polypyrrole (PPy), poly (phenylene vinylene) and poly (p-phenylene) (Heeger, 2001).

One of the shortcomings of CPs is their low conductivity ($< 10^{-5}$ S cm$^{-1}$). Hence, a doping process is necessary to extract the electrons from the backbone of the CPs to increase their electrical conductivity. However, the protonation process is only applicable to polyaniline (PANI). CPs containing positive charges in its backbone are considered to be charge carriers, leading to conducting properties ($1-10^{5}$ S cm$^{-1}$) (Le *et al.*, 2017; Hangarter *et al.*, 2013). Obviously, the resulting conductance is related to the concentration and type of dopants (Abdiryim *et al.*, 2005; Kumar and Sharma, 1998; Chiang *et al.*, 1978). Most CPs, such as PPy and PANI, show p-type semiconducting behavior and are unstable in the un-doped state. The dopants can help maintain charge neutrality and also increase the conductivity (Miasik *et al.*, 1986). The most widely used process for synthesis of CPs is oxidative polymerization of aromatic benzoids (aniline, phenylenevinylene, and diphenylamine) or heterocycles (thiophenes, pyrroles, azines) (Shirakawa *et al.*, 1977). Usually, the monomer is oxidized, and cation radicals are formed. The oxidation can be tracked between two cation radicals by a dimerization reaction. Growth of the chain occurs via the connection of radical ions, as shown in Fig. 2 for pyrrole (Choudhary *et al.*, 2014). The oxidation process could be performed either electrochemically (using anodic polarization on the electrode) or chemically (by adding oxidants). In electrochemical polymerization, the oxidation state can be controlled by the electrode potential, while the chemical route is better for preparing composites or large quantities of polymer (Choudhary *et al.*, 2014).

A protonic acid as oxidant is needed to produce a linear polymer. The most commonly used oxidants are $(NH_4)_2S_2O_8$, $(H_2O_2)$ and $(Ce(SO_4))_2$. Both organic media and aqueous media can be employed for the production of linear polymers. Galvanostatic, potentiostatic, and potentiodynamic methods can be utilized in an elec-

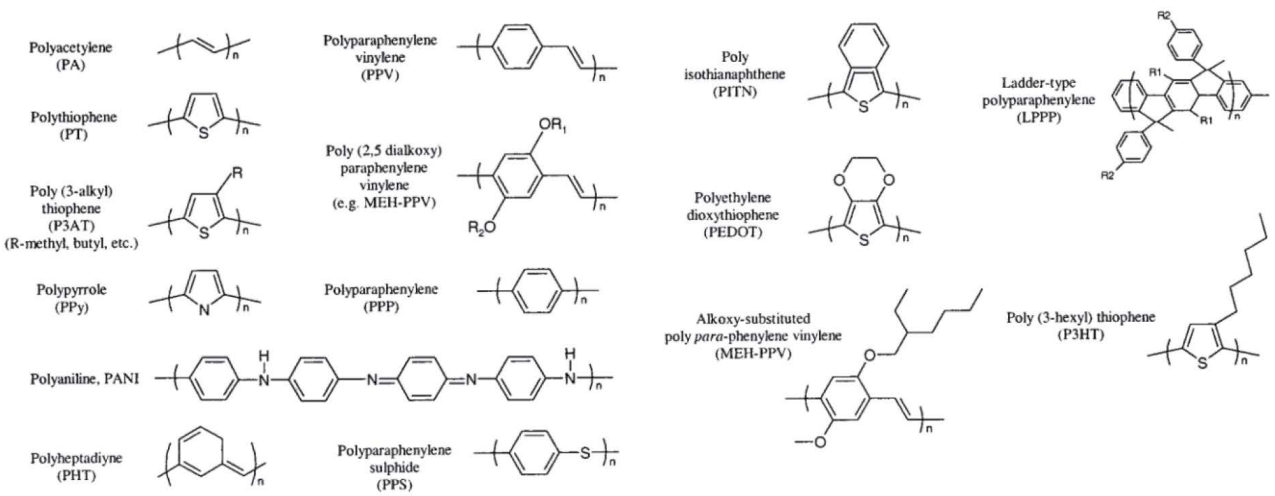


**Fig. 1.** Structure of the most important CPs. Reproduced from (Heeger, 2001), copyright 2020.

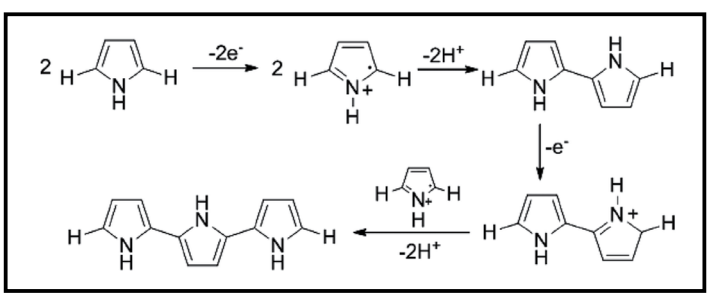


**Fig. 2.** The scheme of pyrrole polymerization mechanism. Reproduced with permission from (Choudhary *et al.*, 2014), copyright 2020.

trochemical process. All methods have three-electrodes: a reference electrode, a counter electrode and a working electrode (Bai and Shi, 2007; Skotheim and Reynolds, 2007). Some CPs such as poly (phenylene ethynylene), poly (phenylene vinylene) and their derivatives have been prepared via other chemical methods instead of oxidation polymerization (Jung *et al.*, 2000; Yang *et al.*, 1995; Gilch and Wheelwright, 1966).

Controlling the morphology and conductivity of CPs strongly depends on the synthesis procedure (Skotheim and Reynolds, 2007). In addition to polymerization and electrochemical techniques, chemical, plasma, photochemical and enzymatic methods can be used to prepare polymer chains from the monomer precursors (Liu *et al.*, 1999; Chandler and Pletcher, 1986; Mohammadi *et al.*, 1986). However, the chemical synthesis method is the preferred method according to literature, followed by electrochemical polymerization. Conducting polymers synthesized using chemical methods require initial solubilization of the polymers and then inkjet coating, drop casting or electrospinning techniques for fabrication (Rojas and Pinto, 2008; Kovtyukhova *et al.*, 2002). However, CP NFs synthesized by electrospinning offer a high surface area, which is a big advantage for sensing studies. Therefore, we discuss the principles of the electrospinning technique for preparation of CPs in the following section.

## 3. ELECTROSPINNING

The electrospinning process is a kind of electrospray process introduced by Formhals in 1934 (Formhals, 1934). Electrospinning is an efficient process that can produce long polymeric NFs (NFs) (Long *et al.*, 2011; Huang *et al.*, 2006). The electrical, magnetic, as well as sensing properties of the resulting NF can be tuned by changing the diameter of synthesized NFs (Wong *et al.*, 2008; Cai and Martin, 1989).

An electrospinning instrument consists of three major parts: a syringe equipped with a pump, a high-voltage system and an electrically grounded collector (Fig. 3) (Ramakrishna *et al.*, 2006). During electrospinning, NFs are produced by applying an electric force to polymer solutions kept inside the syringe. The mechanism of fiber formation is due to "electrostatic attraction" of charges. The solution inside the syringe has a definite surface tension, which is charged by applying a high voltage acting at the tip of the needle. To collect the ejected NFs, the charged collector is placed at a given distance (~10–30 cm) from the tip of the syringe. When a driving voltage (10–30 kV) is applied, the solution in the syringe is ejected by overcoming surface tension and accelerates towards the collector plate, forming a cone-like structure. During this process, the solvent undergoes evaporation and the polymer stretches greatly, leading to the formation of a solid polymer fiber. The produced NFs accumulate on the collector plate and are then collected for further use (Chinnappan *et al.*, 2017; Subbiah *et al.*, 2005).

The fiber morphology is related to the features of environmental conditions, the solution (system parameters) and process conditions (operational parameters) (Teo and Ramakrishna, 2006). Non-woven or uniaxially aligned NFs can be produced in three-dimensional NFs with a huge specific surface area and high porosity (Lim, 2017). NF structures with desirable physico-chemical

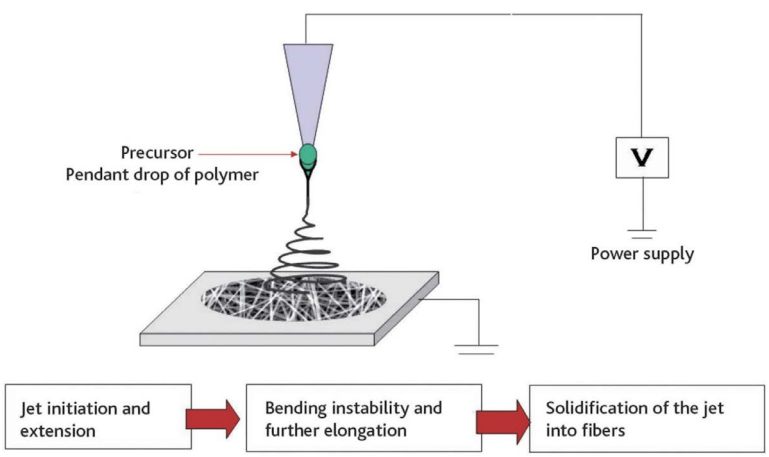


**Fig. 3.** Basic scheme for electrospinning process. Reproduced with permission from Ramakrishna *et al.* (2006).

and electrical properties can be manufactured by electrospinning, and these structures can have an extraordinary effect on the sensing properties (Sun *et al.*, 2003). Moreover, secondary structures of NFs can be controlled to synthesize NFs with core/shell structures (Starr and Andrew, 2013), NFs with hollow structures and NFs with porous structures (Bhardwaj and Kundu, 2010; Sun *et al.*, 2003).

## 3.1 Types of Electrospinning

Different types of electrospinning techniques and instruments are available. However, they differ in the type of collector and spinneret. Some of them use an electrode material as a spinneret, whereas some others are needleless (Afshari, 2016). Co-axial electrospinning, co-electrospinning (Jiang *et al.*, 2005a), multi-needle electrospinning (Tomaszewski and Szadkowski, 2005) and needleless electrospinning (Wang *et al.*, 2009a) are the main types of electrospinning processes. Multi-needle and needleless electrospinning methods are used to improve the efficiency of the traditional electrospinning method. Co-axial electrospinning is utilized to prepare multi-layer and core-shell composite NFs structures with more functionality and better quality (Zhang *et al.*, 2004). In this technique, two discrete NF building blocks are provided via coaxial narrow channels and are synthesized into core-shell NFs (Lim, 2017). Co-electrospinning is also capable of producing single layer and bilayer NFs (Starr and Andrew, 2013). Multi-layer electrospinning can also be utilized to prepare hierarchical NF morphologies (Kayaci *et al.*, 2014; Li *et al.*, 2014; Tran and Kalra, 2013).

## 3.2 Operational Parameters

Structure, porosity, diameter, and surface area play important roles in the final features of the NFs, and fortunately they can be controlled during the electrospinning process (Tan *et al.*, 2005). The parameters involved in the electrospinning method should be carefully optimized to synthesize NFs with better performance in gas sensors. We discuss electrospinning parameters in the following sections. More details can be found in Tan *et al.* (2005).

### 3.2.1 Solution Parameters

#### 3.2.1.1 Concentration of Solution

The optimum solution concentration should be used for the electrospinning process, otherwise beads are formed instead of fibers. A minimum solution concentration for fiber formation is needed. At low solution concentrations, NFs contain beads, and the bead shapes vary from spherical to spindle-like as the solution concentration increases (Tan *et al.*, 2005). The fabrication of continuous fibers at higher concentrations is forbidden due to the inability to maintain solution flow at the tip of the needle (Sukigara *et al.*, 2003).

#### 3.2.1.2 Molecular Weight of CPs

The quantity of entanglements in the polymer chains is influenced by the polymer molecular weight, which changes the characteristics of NFs. Furthermore, it has a remarkable influence on the electrical and rheological features like surface tension, viscosity and conductivity of CPs (Haghi and Akbari, 2007). Polymers with different molecular weights create fibers with different diameters (Liu *et al.*, 1999). Polymers with optimal molecular weights must be selected for producing continuous and smooth NFs (Tan *et al.*, 2005).

#### 3.2.1.3 Viscosity of Solution

These factors greatly affect the morphology of the resulting NFs and should be optimized. If the solution viscosity is too low, electrospraying may occur. Higher viscosity solutions are very hard to force through the needle, resulting in unstable feed rate control of the solution at the tip (Patil *et al.*, 2017; Sukigara *et al.*, 2003).

#### 3.2.1.4 Surface Tension of Solution

Surface tension, which strongly depends on the solvent composition, plays an essential role in the electrospinning synthesis of polymers. Various solvents have various surface tensions. NFs without beads can be made by decreasing the surface tension of the solution. A high surface tension makes the electrospinning method difficult due to the instability of jets and the production of sprayed droplets (Hohman *et al.*, 2001). However, lower surface tensions help make the electrospinning method easier at a lower electric field (Haghi and Akbari, 2007).

#### 3.2.1.5 Solution Conductivity

Jet formation is highly depended on the charged ions in the polymer solution. The final conductivity of the solution depends on the solvent, polymer, and the availability of ionizable salts. Solutions with high conductivity are unstable in the vicinity of severe electric fields,

which results in wide diameter distributions. In contrast, a solution with a low conductivity cannot generate uniform fibers because the electrical force is cannot adequately elongate the fibers (Haghi and Akbari, 2007; Hayati *et al.*, 1987). Electrospun NFs can often be prepared with ultra-small diameters from solutions with high electrical conductivities (Li and Wang, 2013; Huang *et al.*, 2003; Fong *et al.*, 1999).

### 3.2.2 Process Parameters

#### 3.2.2.1 Applied Voltage

The voltage is another key factor during the electrospinning of polymer NFs. Electrostatic interaction forces, due to the applied voltage, will result in the formation of a Taylor cone. When the electrostatic forces are larger than the surface tension force, the ejected Taylor cone is distorted (Kriegel *et al.*, 2008). Electrostatic forces increase as the applied voltage increases, which will result in accelerating the polymer jet. Accordingly, the fiber is stretched, leading to a reduction in the NF diameters (Kriegel *et al.*, 2008; Buchko *et al.*, 1999).

#### 3.2.2.2 Flow Rate

Overall, lower flow rates of the solution favor polarization of the polymer solution. The pore diameter and fiber diameter increase with increasing solution feed rate, and beads appeared on NFs. Flow rates that are too low can increase the overall time of the electrospinning process (Thenmozhi *et al.*, 2017; Chronakis, 2005).

#### 3.2.2.3 Types of Collectors

A conductive substrate is always used as a collector for collecting NFs. Aluminum foil is widely used for the fabrication of collectors due to its low cost, wide availability and ease of modification, which allows the collection of several NFs. Usually collectors in the form of rotating drums are used to create NFs with uniform thickness and excellent reproducibility (Patil *et al.*, 2017). Other occasionally used collectors are conductive cloth, conductive paper, pins (Sundaray *et al.*, 2004), rotating disks (Xu *et al.*, 2004), wire mesh (Wang *et al.*, 2005), and parallel bars (Li *et al.*, 2004).

#### 3.2.2.4 Tip to Collector Distance

One good method to control the morphology and diameter of NFs is to control the tip to collector distance. Generally, there is an optimal distance between the collector and tip that improves the evaporation of NF solutions and accordingly a minimum distance is needed for drying the fiber before it reaches the collector. When the distance is too short or too long, beads can be formed (Xu *et al.*, 2004). Flatter fibers can be generated at closer distances, but rounder fibers form at longer distances (Chronakis, 2005).

### 3.2.3 Ambient Conditions

#### 3.2.3.1 Temperature and Humidity

During the electrospinning method, temperature and humidity also play an essential role in the final properties of synthesized NFs. As temperature increases, the final diameters of the NFs decrease because of increased evaporation of solvent, while the higher humidity will result in the formation of more pores on the surface of NFs (Pillay *et al.*, 2013; Casper *et al.*, 2004).

## 4. CONDUCTIVE POLYMERS AS GAS SENSORS

### 4.1 Sensor Configuration

In resistive-based gas sensors, the electrical resistance greatly depends on the ambient gases in terms of type and concentration (Mirzaei *et al.*, 2016). Such gas sensors are particularly suitable for detecting different gases and concentration variations (Neri and Donato, 1999). Fabrication of the sensor includes the deposition of a sensing layer (CPs) on an alumina, $SiO_2$/Si or flexible substrate that has interdigitated electrodes (e.g., Au, Pt) for reading the sensor resistance. A heater is also used on the back side of the sensor to heat it to the desired sensing temperature.

The electrospun CP-based gas sensors discussed in this review can be used to detect many toxic, VOC, and flammable gases such as $H_2$, $NO_2$, $CO_2$, triethylamine, methanol, and liquefied petroleum gas (LPG). In Table 1, the main source of emission, hazardous effects, and the threshold limit value (TLV) of the most important gases are presented.

### 4.2 General Sensing Mechanism

The sensing capabilities of CPs are due to interactions of the target gas with the CP sensing materials, which can result in changes in conductivity, the doping level and electron transport in the conjugated backbone. It has

**Table 1.** A list of organic compounds detected by resistive CP-based gas sensors.

| Gas | Source of emission or application | Toxicity/Hazardous effects | TLV (ppm) | Ref. |
|---|---|---|---|---|
| Methanol ($CH_3OH$) | Widely used as solvent | Nausea, blurred vision, headaches, eye irritation dizziness drowsiness, dermatitis and scaling. | 200 (ACGIH) | Mirzaei *et al.*, 2016 |
| Triethylamine ($C_6H_{15}N$) | Widely used in catalysts, organic solvents, high energy fuels, preservatives, and bactericides | Explosive and flammable gas that irritates skin and causes asthma, visual disturbances, headaches | 1 (ACGIH) | Xie *et al.*, 2013; Song *et al.*, 2017 |
| LPG | Widely used as a fuel in homes, vehicles and industries | Highly flammable and explosive | 100 (OSHA) | Patil *et al.*, 2015; Yang *et al.*, 2018 |
| 2-propanol ($C_3H_8O$) | Widely used as industrial solvent | Mild irritation to the nose and eyes. Ingestion causes drowsiness, dizziness and nausea. | 400 (ACGIH) | Kumar *et al.*, 2014; Mirzaei *et al.*, 2016 |

OSHA: The Occupational and Safety Health Administration; ACGIH: American Conference of Government Industrial Hygienists.

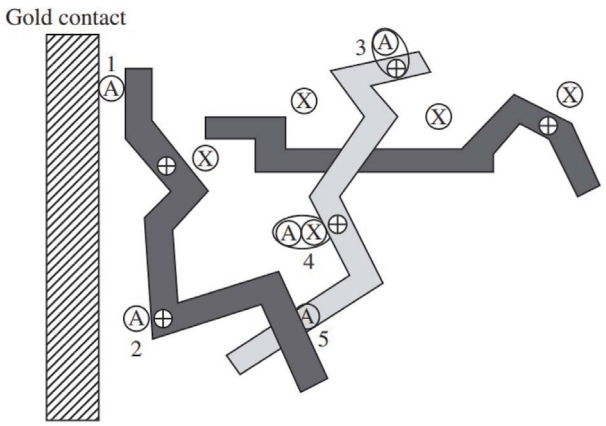


**Fig. 4.** Possible interaction sites for a target gas on a CPs sensing layer. Reproduced with permission from (Neri and Donato, 1999), copyright 2020.

been suggested that there are five possible interactions between the CP NF sensing layer and the target gas that can alter the conductance (Neri and Donato, 1999), as shown in Fig. 4. First, such a response may be caused by how the target gas affects the charge transfer between the electrode and CP. Second, this response may be due to direct creation or elimination of the charge carriers, e.g., via oxidation or reduction of the polymer chain. In particular, this interaction may be significant for $NH_3$, although this seems less likely for weakly interacting organic vapors such as alcohols (Wetchakun *et al.*, 2011; Gardner and Bartlett, 2000). Third, the charge carrier mobility in a polymer chain can be altered via interactions between the mobile charge carriers and the target gas across the polymer chains. Fourth, the target gas can interact with counter ions ($X^-$) in the sensing layer, thus altering the mobility of the charge carriers along the polymer chain. Counter ions with relatively low mobility are generally connected in the polymer chains. The target gas diffuses into the polymer film and acts as a solvent for the counter ions, resulting in ionic conduction (Dixit *et al.*, 2005). Finally, the target gas can modulate the resistance of a CP film by affecting the rate of interchain hopping.

Electron transfer is the general sensing mechanism in CP-based gas sensors. Gases with an electron acceptor nature like $NO_2$ can eliminate electrons from CPs. It is well-known that at low temperatures ($<100°C$), $O_2^-$ is the dominant chemisorbed oxygen type on the surfaces of most sensing materials. First, oxygen gas is adsorbed on the surface of the sensor and then (by taking of electrons from the surfaces of the sensor), it becomes adsorbed in the form of a molecular ion: $O_2 + e \rightarrow O_2^-$. By exposing CP-based gas sensors to a reducing target gas, the target gas molecules can react with the oxygen species and transfer electrons back to the conduction bands of the sensor. Such electrons transferred in the conduction band can be combined with holes from the valence band, thus leading to higher resistances and lower carrier concentrations for the CP gas sensors. In addition, the resistance decreases for oxidizing gases. However, a signal can appear in both cases. At room temperature, this type of mechanism may contribute less to the sensor signal in CP-based gas sensors, as the concentration of $O_2^-$ is generally very low at room temperature

(Densakulprasert *et al.*, 2005).

Occasionally, a noble metal catalyst like Pd, Au, or Pt is added to the CP film, which allows for the detection of various less reactive gases (Shirsat *et al.*, 2009). Noble metals can catalytically decompose and increase the adsorption of target gases via a spill over process. Furthermore, since the work functions of noble metals and CPs are different, heterojunctions can form between a noble metal and a CP, which can change the resistance of the sensor by modulating the height of the potential barrier formed in the presence of target gases. Hybrid composites of CPs and n-type metal oxides show synergic interactions between the CPs and metal oxides, resulting in the generation of p-n junctions. For example, in a hybrid consisting of PPy (which is a p-type material) and $WO_3$ (which is an n-type material), the p-n junctions formed in the PPy-$WO_3$ p-n heterojunctions can enhance the depletion barrier height, resulting in changes in the sensor response (Sun *et al.*, 2017). Swelling is another mechanism present in CP-based gas sensors (Thenmozhi *et al.*, 2017); as the gas molecules diffuse into the polymer chains, electron hopping becomes difficult because of the increased distance between polymer chains resulting from swelling. Swelling can disrupt conductive pathways in the CP film and increase the sensor resistance when the desired gas is injected, thus enhancing the gas response of the sensor (Guernion *et al.*, 2002).

In the next sections, we analyze how the above gas sensing mechanisms can explain the sensing behavior of CP-based gas sensors. The sensing parameters (e.g., sensing range, sensitivity, DL, response time, and selectivity) of all the covered CPs-based sensors are shown in Table 2.

### 4.3 Polyaniline (PANI)-based NF Gas Sensors

Among many CPs, PANI has been the most studied material due to its various characteristics such as reversible doping, dedoping, tunable electrical conductivity, high environmental stability and easy preparation (Sen *et al.*, 2016). PANI can be synthesized using the oxidizing polymerization of aniline from two structural units, i.e., a reduced (B-NH-B-NH) unit and an oxidized (B-N=Q=N$^-$) unit, where B is denoted as a benzenoid and Q is denoted as a quinoid ring.

PANI has the ability to undergo reversible doping under acidic (proton doping) or basic conditions. When PANI is doped with an acid, the imine nitrogen of the polymer backbone is protonated to induce charge carriers. In this situation, the electrical conductivity of PANI increases ($\sigma > 1$ S cm$^{-1}$), and this doped form of PANI is known as an emeraldine oxidation state or emeraldine salt (Fig. 5). The un-doped polymer chain is known as an emeraldine base ($\sigma < 1 \times 10^{-10}$ S cm$^{-1}$) (Fratoddi *et al.*, 2015; Huang *et al.*, 2004).

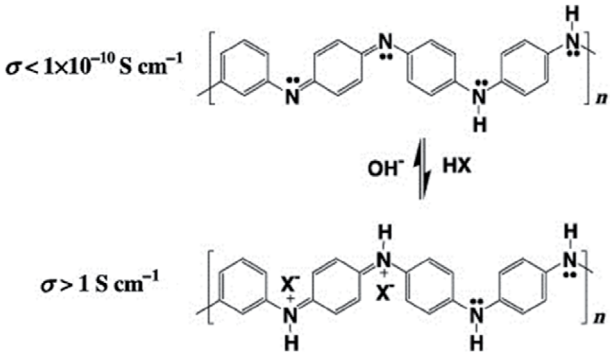


**Fig. 5.** Repeat unit of the emeraldine oxidation state of polyaniline in the un-doped base form (top) and the fully doped, acid form (bottom). Reproduced with permission from (Huang *et al.*, 2004) from Springer, copyright 2020.

Various nanostructures of PANI including NFs, nanotubes, and nanoparticles have been synthesized by numerous of methods (Kumar *et al.*, 2017, 2016; Gu *et al.*, 2014; Ayad *et al.*, 2013; Long *et al.*, 2011; Rahy and Yang, 2008). These morphologies have high exposed surface area (e.g., PANI NFs with 50 nm diameter have 49.3 m$^2$/g surface area), which can facilitate gas molecules adsorption and greater penetration into the pores (Huang *et al.*, 2004). Introducing a secondary component to the primary PANI nanostructures further enhances its sensing properties due to the synergistic effect between both the components. Various materials such as metallic nanoparticles, metal-oxides, carbon-based materials (CNT, Graphene), and polymers have been added to PANI to tune the sensitivity and selectivity properties (Park *et al.*, 2017). In this section, we discuss gas sensors based on PANI NFs as a sensing layer in their pristine or composite form.

For the sensing of $H_2$, PANI NFs were fabricated as a resistive sensor on Pt or Au electrodes (Fowler *et al.*, 2009). The responses ($R_g/R_a$) of the sensors with Pt and Au electrodes were 1.65 and 1.03, respectively. The reason for the low sensor response on an Au electrode is the interaction between hydrogen and PANI NFs. The high response of the sensor on Pt electrodes is because of interactions with Pt at the PANI-Pt interface. Hydrogen

**Table 2.** Sensing parameters of different CPs-based sensors for the sensing of diverse gases.

| S. No. | Type of CP | Analyte gas | Sensing range | Sensing mechanism | DL | Sensitivity | Response time | Selectivity | Ref |
|---|---|---|---|---|---|---|---|---|---|
| **PANI-based** | | | | | | | | | |
| 1 | PANI NFs | $H_2$ | 10 ppm | Formation of hydride with the platinum | 10 ppm | 2.5% for 10 ppm $H_2$ | | | Fowler *et al.*, 2009 |
| 2 | CSA-doped PANI NF thin films | $H_2$ | 0.1%–1% | Doping-dedoping in PANI | | 1.03 for 10000 ppm of $H_2$ | | | Virji *et al.*, 2006 |
| 3 | HCl-doped PANI | $H_2$ | 0.06%–1% | Protonation of PANI | | 1.11 for 1% $H_2$ | 32 s | | Sadek *et al.*, 2007 |
| 4 | Dedoped PANI | $H_2$ | 0.06%–1% | Protonation of PANI | | 1.07 for 1% $H_2$ | 28 s | | Sadek *et al.*, 2007 |
| | $SnO_2$/Polyaniline | $H_2$ | 1000 and 2000 ppm | Interaction of $H_2$ molecules with depletion region and act as a dielectric between the PANI and $SnO_2$ border | | 4.5 for 2000 ppm $H_2$ | 3 s | | Sharma *et al.*, 2015 |
| 5 | Graphene/PANI | $H_2$ | 0.06%–1% | Depletion of holes from the valence band of graphene and formation of N-H bonds in PANI | | 16.57% for 1% $H_2$ | | | Al-Mashat *et al.*, 2010 |
| 6 | Pd-PANI-rGO | $H_2$ | 0.01–2 vol% | Increase in resistance in presence of $H_2$ | 0.01 vol% | 25 for 1 vol% $H_2$ | 20 s | Selective over $CH_3OH$, $CO_2$, and $H_2S$ | Zou *et al.*, 2016 |
| 7 | PANI/Zinc-based zeolitic benzimidazolate framework | $H_2$ | $0.6–3.0 \times 10^{-3}$ M | Protonation and de-protonation in PANI | 5.27 μM | 11.9 μA mM $H_2$ | 4 s | | Mashao *et al.*, 2019 |
| 8 | PANI/$TiO_2$ NFs | $CO_2$ | 1000 ppm | p-n junction based reduction in activation energy for $CO_2$ | Not provided | | 80 s | Not tested | Nimkar *et al.*, 2015 |
| 9 | CLBC-AmG/PANI | $CO_2$ | 50 to 2000 ppm | p-n junction based | ~26.55 ppm | | 20 s | Selective in presence of 550 ppm $NH_3$, $H_2$, and CO | Abdali *et al.*, 2019 |
| 10 | PANI/PLFO | $CO_2$ | 5000–20000 ppm | Protonation and de-protonation | | 44.9 for 20000 ppm $CO_2$ | 101.37 s | | Hashemi Karouei and Milani Moghaddam, 2019 |
| 11 | PANI/PEO | LPG | 1000 ppm | Transfer of electrons from PANI to LPG | Not provided | 7.33% | 110 s | Not tested | Patil *et al.*, 2015 |
| 12 | PANI/ZnO/PEO | LPG | 1000 ppm | Transfer of electrons from PANI to LPG | Not provided | 8.73% | 100 s | Not tested | Patil *et al.*, 2015 |
| **PPy-based** | | | | | | | | | |
| 1 | PAN/Tos-PPy | $CH_3OH$ | 0.7–6.5% | Dedoping reaction between methanol and Tos-PPy | | 7.5% for 3.4% methanol | 20 s | | Jun *et al.*, 2013 |
| 2 | PPy/PVA | $CH_3OH$ | 49–1059 ppm | Donation of electron from alcohol to p-type PPy | | 2.6% for 49 ppm | 304 s | | Jiang *et al.*, 2005b |
| 3 | PPy/PVA | Ethanol | 100 ppm | Formation of N-H partial bond | | 72% for 100 ppm ethanol | 42 s | Selective over 100 ppm of ammonia, toluene, chloroform, and acetone vapors | Das and Sarkar, 2018 |

**Table 2.** Continued.

| S. No. | Type of CP | Analyte gas | Sensing range | Sensing mechanism | DL | Sensitivity | Response time | Selectivity | Ref |
|---|---|---|---|---|---|---|---|---|---|
| 4 | Ag NPs deposited rod-like PPy | Acetone | 195–580 ppm | Doping-dedoping in PPy | 25 ppm | | 280 s | Selective over propanol, water, and formaldehyde | Adhikari *et al.*, 2020 |
| 5 | PPy | $H_2$ | | | | 1.12 for 10000 ppm $H_2$ gas | | | Al-Mashat *et al.*, 2008 |
| 6 | Pd nanoparticles modified PPy films | $H_2$ | 100 to 5000 ppm | Catalytic properties of Pd nanoparticles and increase in the number of delocalized charge carriers on PPy | | 42 for 20 ppm $H_2$ gas | 6.5 s | Selective over 20 ppm of $NH_3$, 200 ppm of CO, and 5 ppm $NO_2$ gas | Su and Liao, 2016 |
| **PEDOT-based** | | | | | | | | | |
| 1 | PEDOT-PSSA | Methanol, ethanol, propanol, $NH_3$, HCl, and $NO_2$ gas | $1.28 \times 10^5$ ppm for methanol, $6 \times 10^4$ ppm for ethanol, $1.3 \times 10^4$ ppm for 2-propanol, $1.5 \times 10^5$ ppm for $NH_3$, $2.47 \times 10^5$ ppm for HCl, and $1 \times 10^3$ ppm for $NO_2$ | Polymer swelling for methanol, ethanol, and 2-propanol De-dpoing/doping for $NH_3$, HCl, and $NO_2$ | Not provided | | 8 s for methanol, 10 s for ethanol, 20 s for 2-propanol, 13 s for $NH_3$, 95 s for HCl, and 120 s for $NO_2$ | Not tested | Pinto *et al.*, 2011 |
| 2 | $Ti_3C_2T_x$/PEDOT/PSS | $CH_3OH$ | 180–500 ppm | Donation of electron by analyte gas to sensing material | | 1.6 for 500 ppm $CH_3OH$ | | Selective over acetone and ethanol | Wang *et al.*, 2019 |
| 3 | PEDOT | $NO_2$ | 10–100 ppm | Oxidation of PEDOT by $NO_2$ gas | | 22% for 100 ppm $NO_2$ | 60 min | Selective over 100 ppm of $NH_3$, $H_2S$ and $SO_2$ | Dunst *et al.*, 2017 |
| 4 | PEDOT-PSS/$TiO_2$ | Oxidized NO | 10–130 ppb | Reduction in the depletion region of p-n junction | 1 ppb | $2.9 \pm 0.1 \times 10^3$ $ppb^{-1}$ | 5–17 min | In presence of $H_2O$, $CO_2$, and $O_2$ | Zampetti *et al.*, 2013 |
| 5 | $WO_3$-PEDOT : PSS | $NO_2$ | 50–200 ppb | Interaction of $NO_2$ gas with the p-n junction | 30 ppb | ~1.2 for 50 ppb $NO_2$ | 45.1 s | Selective over $NH_3$, $H_2$, ethanol, methanol, and acetone | Lin *et al.*, 2015 |
| 6 | PEDOT-graphene | $NO_2$ | 5–100 ppm | Increase in number of charge carriers in rGO and PEDOT due to $NO_2$ interaction | | | 3 min | Displayed much higher response in comparison to 100 ppm of $NH_3$, $H_2S$ and $SO_2$ | Dunst *et al.*, 2016 |

helps to form a Schottky barrier between Pt and PANI via a variation in the work function as Pt was changed to Pt hydride. The formation of a hydride between the PANI NF layer and the platinum electrode resulted in non-ohmic behavior in the Pt-PANI NFs upon exposure to a $H_2$ environment. Pt is introduced to make a platinum hydride in contact with $H_2$ gas.

The mechanism of hydride formation is shown in Fig. 6. The sensor includes a porous mesh of PANI NFs on Pt electrodes (Fig. 6a). When this sensor is in contact with $H_2$, the gas passes through PANI and reaches the Pt surfaces (Fig. 6b–d). However, some of the hydrogen can also react with PANI before reaching the Pt. Platinum hydride ($PdH_x$) is produced at the interface of the PANI NFs and the platinum metal. When the PANI NFs mesh is exposed to oxygen, it reacts with the $PdH_x$ surface. Water and Pt metal form due to the elimination of hydride. Because the work function for PANI NFs is between the work functions for Pt and $PdH_x$, $H_2$ results in the formation of a Schottky barrier, which is the main reason for the sensitivity of the Pt-PANI NFs gas sensor. The hydrogen exposure results in large changes in the work function of the Pt contact. Metal hydride cannot form on Au electrodes, and ohmic contacts with the PANI NFs are formed, and only the interaction between PANI NFs and $H_2$ are observed. The small change in resistance is due to binding between $H_2$ and PANI NFs. In fact, platinum hydride forms via the Pt-PANI NF-hydrogen interactions, and Pt hydride formation is the main reason for the improved sensor response.

In another work, camphorsulfonic acid (CSA) doped PANI NF thin films were utilized for sensing of hydrogen (Virji *et al.*, 2006). The resistance change of PANI NFs was greater than conventional PANI due to their porous structure backbone that leads to enhanced diffusion of gas into the film. Hydrogen gas sensing studies showed that the response ($R_a/R_g$) of the gas sensor was 1.03 for 10000 ppm $H_2$ gas. Fig. 7 shows a gas sensing mechanism for the interaction of $H_2$ with PANI. $H_2$ interacts with doped PANI at the charged amine nitrogen sites. Formation of new N-H bonds to the amine nitrogen of the PANI chains lead to dissociation of $H_2$ bonds. This reaction is quite reversible because charge transfer among adjoining amine nitrogen groups brought the PANI back to its doped, polaronic, emeraldine salt state free of $H_2$. This mechanism just occurs in the emeraldine salt form of PANI.

The PANI base emeraldine form is electrically insulating. Thus, there is no transfer of charge among the nitrogen units on the PANI chain, hindering the interactions between $H_2$ and the polymer. In other words, the response of dedoped PANI towards hydrogen is negligible since hydrogen cannot dissociate to interact with the dedoped PANI. The presence of water can also significantly decrease the response of a sensor for hydrogen. Since water molecules have a high affinity to bond with the nitrogen atoms of PANI, the available sites for adsorption of hydrogen decrease, resulting in a low response of sensors to hydrogen. The doping and dedoping in PANI is the crucial for the sensing of $H_2$. In a report on conductometric $H_2$ sensor, it was observed

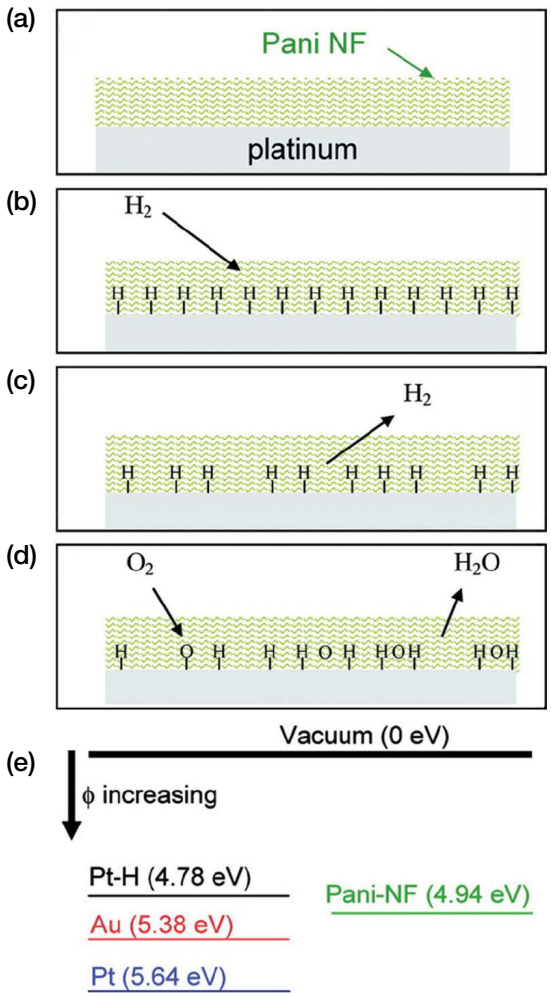


**Fig. 6.** Interaction of PANI-coated platinum-based sensor with the $H_2$ gas. (a) Sensor structure and (b–d) interaction of hydrogen and oxygen on the surface of sensor. (e) Work functions of Pt, Au, $PtH_x$. Reprinted with permission from (Fowler *et al.*, 2009). Copyright (2020) American Chemical Society.

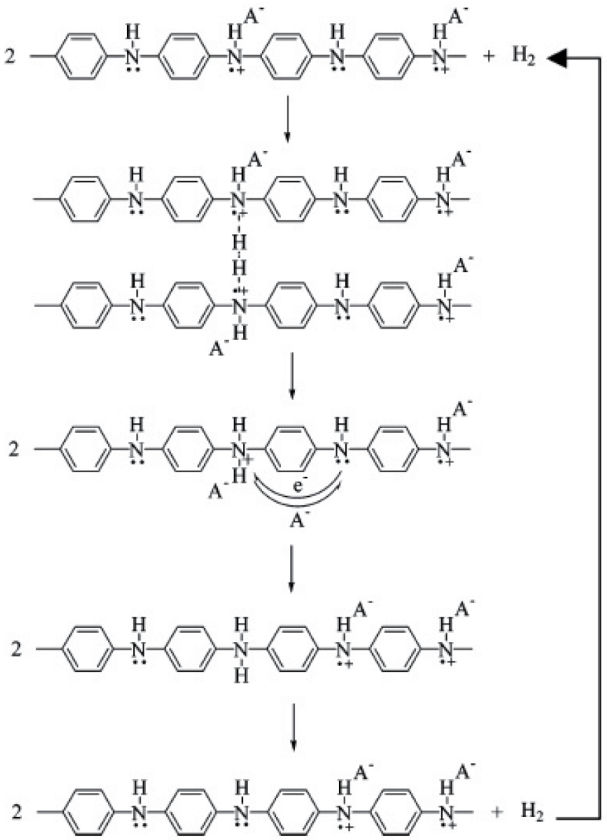

**Fig. 7.** Possible mechanism for hydrogen interaction with doped PANI, where A represents the counteranion. Reprinted with permission from (Virji *et al.*, 2006), copyright (2020) American Chemical Society.

that the doped form of PANI displayed higher sensitivity in comparison to the dedoped PANI. Nonetheless, the dedoped PANI-based $H_2$ sensor outperformed doped PANI in terms of repeatability and baseline stability (Sadek *et al.*, 2007). The composite forms of PANI are also found excellent in improving the $H_2$ sensing capabilities of PANI. In particular, the composites of PANI with graphene-materials (e.g., reduced graphene oxide; rGO), metal organic frameworks (MOFs), and $SnO_2$ displayed good performance for the sensing of $H_2$ gas (Mashao *et al.*, 2019; Zou *et al.*, 2016; Sharma *et al.*, 2015; Al-Mashat *et al.*, 2010). The performance of these sensors can be accessed from Table 2.

The conductivity of PANI composites may increase by including metallic particles or acidic or oxidative doping (Ayad and Zaki, 2008). The selectivity of PANI gas sensors may increase by adding different kinds of dopants like protonic acids (Samui *et al.*, 2001), surfactants (Stejskal *et al.*, 2003) and metals (Wong *et al.*, 2019). Mixing PANI with nanosized metal oxides can increase the selectivity and sensitivity of the CPs. The sensors worked at ambient temperature, and the selectivity to different gases could be improved by increasing the concentration of nanosized metal oxides. Nimkar *et al.* (2015) prepared $TiO_2$ incorporated PANI NFs using the electrospinning technique. The NFs of the PANI/$TiO_2$ nanocomposite showed a good response ($R_g/R_a$) of ~2.68 towards 0.1% $CO_2$ gas at 48°C. Also, the response time of the PANI/$TiO_2$ NFs film for 0.1% $CO_2$ gas was ~80 s. When PANI/$TiO_2$ NFs films were exposed to $CO_2$ gas, the gas penetrated into the PANI matrix, and the improved sensitivity of this sensor was related to the formation of a positively charged depletion layer. Electron transfer from $TiO_2$ to PANI occurs at the heterojunction. As a result, the activation energy and enthalpy of physisorbed $CO_2$ gas decreased. The excellent reversibility and the short response time of the PANI/$TiO_2$ NFs layer is due to the surface morphologies of NFs. Specifically, the gas can diffuse in a NF structure more easily, resulting in large exposure regions and high penetration depths for gas molecules. As shown in Table 2, the composites of PANI with other potential structures, e.g., cross-linked bacterial cellulose-amino graphene (CLBC-AmG) and $LaFeO_3$ microsphere (PLFO) are also efficient for the sensing of $CO_2$ (Abdali *et al.*, 2019; Hashemi Karouei and Milani Moghaddam, 2019).

Hybridization of CPs and metal oxides can enhance the features of the resulting gas sensor, and newly fabricated materials demonstrate the synergistic results of these two materials. In an interesting study, electrospun D-camphor-10-sulphonic acid (CSA) doped PANI/polyethylene oxide (PANI/PEO) and PANI/ZnO/PEO NFs were synthesized (Patil *et al.*, 2015). A sol-gel method was employed for the synthesis of ZnO NPs. PANI (in the form of emeraldine base) and PANI/ZnO were prepared by chemical oxidative polymerization with CSA to improve conductivity and solubility. These were mixed with PEO solutions to obtain NFs by the electrospinning method. The LPG sensing capabilities of the sensors were tested at 30–90°C, and the optimal sensing temperature was 36°C, which is a safe temperature for LPG detection due to the explosive nature of LPG gas. The LPG gas sensing results showed that PANI/ZnO/PEO sensors had a higher response to LPG relative to PANI/PEO sensors. In particular, the responses ($R_g/R_a$) to 1000 ppm LPG were 1.087 and 1.073 for the PANI/

ZnO/PEO and PANI/PEO gas sensors, respectively. CPs are often doped/undoped by redox reactions. Thus, transferring electrons can change the doping level and alter the resistance and work function of the CPs. The transfer of electrons happens when PANI and PANI/ZnO composite NFs were in contact with LPG gas. Electron acceptors remove electrons from PANI, resulting in an increased doping level and electrical conductivity in p-type CPs. In contrast, when an electro-donating gas such as LPG is used, the doping level of PANI decreases, thus changing the resistance of the sensor. Also, in PANI/ZnO/PEO NFs, p-n heterojunctions lead to additional resistance modulation, resulting in enhanced gas sensing. The other mechanism is the alteration of physical properties of the polymers such as crystallinity and morphology, which alter the electrical resistance via an increase in electron transfer. In such a case, the sensitivity of the sensor in the presence of LPG is related to adsorption on a polymer surface via diffusion to inner-domain spaces.

### 4.4 Polypyrrole (PPy)-based NF Gas Sensors

After PANI CPs, polypyrrole (PPy) is highly popular due to its easy synthesis via chemical or electrochemical oxidation polymerization, high electrical conductivity and high stability. The material and sensing properties of PPy can be enhanced by combining it with additional inorganic or organic components. Usually a doped PPy behaves like a p-type semiconductor, where a change in conductivity occurs through interactions with a target gas (Joshi *et al.*, 2011; Kim and Yoo, 2011; Yoon *et al.*, 2006; Penza *et al.*, 1997). Lots of PPy composite materials have been reported for gas sensing applications for a wide range of gases or vapors such as $NO_2$, $H_2S$, water, and VOCs (Su and Shiu, 2011; Geng, 2010; Wang *et al.*, 2009b; Han and Shi, 2007; Geng *et al.*, 2006; Tandon *et al.*, 2006; An *et al.*, 2004; Bhat *et al.*, 2003).

A highly porous core-shell polyacrylonitrile-(Tos doped) PAN-PPy NF mat was fabricated as a methanol sensor through electrospinning and two-step vapor-phase polymerization (Jun *et al.*, 2013). The results demonstrated that very thin (~10 nm) conductive PPy shell layers were deposited on electrospun PAN NFs with a median diameter of 258 nm. The PAN-PPy gas sensor revealed a response ($R_g/R_a$) of 1.4 to 10000 ppm methanol at room temperature. The resistance increase upon exposure to methanol was explained by the electron donating character of the $CH_3OH$ gas and the p-type semiconducting nature of PPy. The interactions between Tos-doped PPy and $CH_3OH$ might be described by the redox (dedoping) reaction: $PPy^+/Tos^- + CH_3OH\ (\delta^-) \leftrightarrow [PPy\text{-}CH_3OH\ (\delta^-)]^+/Tos^-$. Likewise, PPy-based materials (e.g., poly (vinyl alcohol) (PVA), silver nanoparticle (Ag NPs), and plastic optical fiber (POF)) are also an effective option to sense other oxygen-containing VOCs, e.g., ethanol and acetone (Table 2) (Adhikari *et al.*, 2020; Liu *et al.*, 2020; Das and Sarkar, 2018; Jiang *et al.*, 2005b).

The transfer of electrons from electron-donating $CH_3OH$ to the positively-charged PPy backbone led to the formation of neutral polymer chains, resulting in a reduction in the hole carrier density (i.e., a resistance increase). In another study (Al-Mashat *et al.*, 2008), PPy NFs were prepared through a simple chemical method for the detection of hydrogen at different temperatures. The preparation of PPy NFs was completed using bipyrrole to accelerate the polymerization of pyrrole with iron chloride as the oxidizing agent. The effects of temperature (up to 100°C) on the $H_2$ sensing properties were studied. At higher working temperatures (>70°C), the response was low ($R_a/R_g = 1.07$ for 10000 ppm $H_2$ at 75°C) because a lot of carriers with high energy moved freely in the polymer chain, preventing the polymer from exhibiting its inherent redox reaction behavior. In addition, the nanostructured PPy film was smoother at high temperatures and included a dense NF morphology that had less porosity relative to the film at lower temperatures, which led to improved conductivity due to enhanced charge carrier hopping between localized states in the polymer chains. The high conductivity of the nanostructured PPy layer decreased the response at high temperatures because the gas molecules could not deeply penetrate into the bulk of the sensor. Accordingly, the sensor showed its maximum response ($R_a/R_g = 1.12$ to 10000 ppm $H_2$ gas) at ambient temperature. A dynamic response was produced because of the interactions between the adsorbed hydrogen gas molecules and the polymer film. This interaction led to a heterogeneous charge transfer reaction, and chemical modulation of the polymer doping level, which depends on the Fermi level of the sensing film. This can cause a shift in the work function or electrical conductivity of the organic film. In terms of the work function, the polarity of the response relates to the ability of the diffusing gas to shift charge density with the polymer matrix by reduction or oxidation reactions. Hydrogen behaves as a reducing gas, so

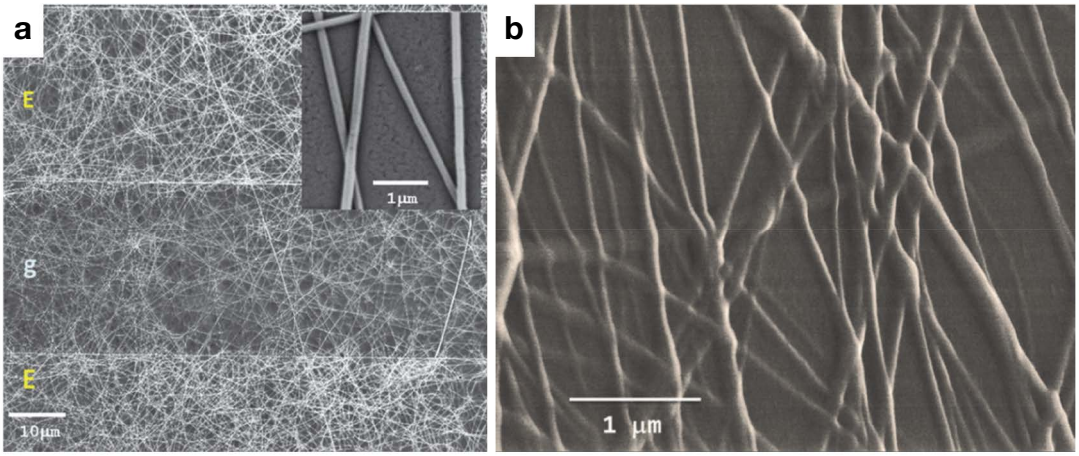


**Fig. 8.** Scanning electron microscopic images of (a) $TiO_2$ electrospun fibrous on IDE and (b) PEDOT-PSS coated $TiO_2$ fibers. E and g in Figure A represents electrode and gap between electrodes, respectively. Reprinted with permission from Zampetti *et al.*(2013).

the PPy NFs resistance decreased when in contact with $H_2$ gas. However, the large variation in its electrical resistance is due to the redox reaction of PPy. The modification of PPy with Pt and Pd nanoparticles have also been tested for the sensing of $H_2$ gas (Su and Liao, 2016). Out of both types of sensors, the sensor developed using Pd nanoparticles modified with PPy exhibited superior sensing characteristics. Such modification led to the formation of more catalytically active sites for the $H_2$ gas molecules. The performances of PPy-based $H_2$ gas sensors are displayed in Table 2.

### 4. 5 PEDOT based NF Gas Sensor

Electrospun NFs of poly(3,4-ethylenedioxythiophene) doped with (polystyrene sulfonic acid)-PEDOT-PSSA were synthesized to sense methanol, ethanol, and 2-propanol vapors (Pinto *et al.*, 2011). Due to the large surface to volume ratio, the sensors had higher sensitivity and faster response times compared to other PEDOT-based alcohol sensors. The sensing mechanisms were related to polymer swelling that increased the inter-chain distance, which reduced the hopping rate. The response times for sensing of methanol, ethanol and 2-propanol were 8, 10 and 20 s, respectively, which are relatively fast for room temperature sensors. Zampetti *et al.* (2013) prepared PEDOT-PSS/$TiO_2$ NFs for $NO_2$ gas sensing (Fig. 8). The sensor detected 20 ppb $NO_2$ in the presence of 40 RH% at room temperature with a response ($I_g/I_a$, where $I_a$ and $I_g$ are the electrical current of the sensor in the presence of air (reference current) and $NO_2$ gas, respectively) of 1.045. The sensing mechanism was mainly related to the change in electrical resistance of the sensor at the interface between CP and $TiO_2$, where the $NO_2$ gas is able to easily alter the resistance of the formed p-n heterojunction. Some other PEDOT-based hybrid structures (e.g., $Ti_3C_2T_x$/PEDOT : PSS) are also explored for the sensing of methanol (Wang *et al.*, 2019).

The same group used electrospinning to fabricate sensing materials via a $TiO_2$ NF scaffold to support a CP (PEDOT: PSS), which resulted in a sensitive membrane (Zampetti *et al.*, 2013). It showed a response ($I_g/I_a$) of 0.5 ppm $NO_2$ gas at ambient temperature. In the presence of 8 RH% it was 1.25. This outcome is related to the competitive nature of absorption/desorption between $H_2O$ vapor and $NO_2$ gas, which decreased the available adsorption sites needed for effective adsorption of $NO_2$ gas. The other PEDOT-based materials (e.g., $WO_3$-PEDOT/PSS and PEDOT-graphene) have also tested successfully for the fabrication of $NO_2$ gas sensors (Dunst *et al.*, 2017, 2016; Lin *et al.*, 2015).

## 5. CONCLUSIONS AND OUTLOOK

Recently, CPs have received much attention for the realization of resistive gas sensors working at low or room temperatures. We discussed the gas sensing performance of electrospun CPs. Electrospun CPs having a high surface area can offer many adsorption sites for effective adsorption of gases. Consequently, they can offer much higher sensitivity to toxic gases compared with thin film sensors. However, because of the room-

temperature or low-temperature working temperature, the response and recovery times of CP-based gas sensors are generally longer than that of metal oxide-based gas sensors. So, most researchers have explored composites of CPs with metal oxides to enhance the resulting gas sensing properties.

Among different CPs, most studies have focused on the sensing characteristics of PANI, PPy and PEDOT. This is due to their advantages like low price, high stability and high conductivity. However, most PANI-based sensors suffer from resistance drift and poor recovery time. Flexible CP-based gas sensors would be promising for future gas sensing technologies. With further advancements in synthesis procedures and discovery of novel CPs, electrospun CP NFs will become some of the most promising candidates for realizing different kinds of gas sensors. However, the major challenge for electrospinning process is its complexity. A complex set-up is required to generate electrospun NFs. Moreover, high power requirement for the generation of NFs is another factor which make electrospinning process more complex.

The electrospun CPs-based gas sensors should be tested on diverse environmental conditions before final implementation. Moreover, by considering the high potential of CPs, CP-based sensors should also be tested for the possible expansion of their applicabilities to cover other types of analytes, e.g., semi-VOCs and aerosols.

## ACKNOWLEDEGEMENT

This work was supported by an Inha University Research Grant. KHK acknowledges support provided by a grant from the National Research Foundation of Korea (NRF) funded by the Ministry of Science, ICT & Future Planning (Grant No: 2016R1E1A1A01940995).

## CONFLICTS OF INTEREST

The authors declare no conflict of interest, and the sponsors had no role in the design of the study, in the collection, analyses, or interpretation of data, in the writing of the manuscript, or in the decision to publish the results.

## REFERENCES

Abdali, H., Heli, B., Ajji, A. (2019) Cellulose Nanopaper Cross-Linked Amino Graphene/Polyaniline Sensors to Detect $CO_2$ Gas at Room Temperature. Sensors, 19(23), 5215. https://doi.org/10.3390/s19235215

Abdiryim, T., Xiao-Gang, Z., Jamal, R. (2005) Comparative studies of solid-state synthesized polyaniline doped with inorganic acids. Materials Chemistry and Physics, 90(2–3), 367–372. https://doi.org/10.1016/j.matchemphys.2004.10.036

Adhikari, A., Kar, P., Rana, D., De, S., Nath, J., Dutta, K., Chattopadhyay, D. (2020) Synthesis of sodium cholate mediated rod-like polypyrrole-silver nanocomposite for selective sensing of acetone vapor. Nano-Structures & Nano-Objects, 21, 100419. https://doi.org/10.1016/j.nanoso.2019.100419

Afshari, M. (2016) Electrospun nanofibers. Woodhead Publishing.

Al-Mashat, L., Shin, K., Kalantar-zadeh, K., Plessis, J.D., Han, S.H., Kojima, R.W., Kaner, R.B., Li, D., Gou, X., Ippolito, S.J., Wlodarski, W. (2010) Graphene/Polyaniline Nanocomposite for Hydrogen Sensing. The Journal of Physical Chemistry C, 114(39), 16168–16173. https://doi.org/10.1021/jp103134u

Al-Mashat, L., Tran, H.D., Wlodarski, W., Kaner, R.B., Kalantar-Zadeh, K. (2008) Conductometric hydrogen gas sensor based on polypyrrole nanofibers. IEEE Sensors Journal, 8(4), 365–370. https://doi.org/10.1109/JSEN.2008.917476

An, K.H., Jeong, S.Y., Hwang, H.R., Lee, Y.H. (2004) Enhanced sensitivity of a gas sensor incorporating single-walled carbon nanotube-polypyrrole nanocomposites. Advanced Materials, 16(12), 1005–1009. https://doi.org/10.1002/adma.200306176

Arafat, M., Dinan, B., Akbar, S.A., Haseeb, A. (2012) Gas sensors based on one dimensional nanostructured metal-oxides: a review. Sensors, 12(6), 7207–7258. https://doi.org/10.3390/s120607207

Ayad, M., El-Hefnawy, G., Zaghlol, S. (2013) Facile synthesis of polyaniline nanoparticles; its adsorption behavior. Chemical Engineering Journal, 217, 460–465. https://doi.org/10.1016/j.cej.2012.11.099

Ayad, M.M., Zaki, E.A. (2008) Doping of polyaniline films with organic sulfonic acids in aqueous media and the effect of water on these doped films. European Polymer Journal, 44(11), 3741–3747. https://doi.org/10.1016/j.eurpolymj.2008.08.012

Azad, A., Akbar, S., Mhaisalkar, S., Birkefeld, L., Goto, K. (1992) Solid-state gas sensors: A review. Journal of the Electrochemical Society, 139(12), 3690–3704.

Baharuddin, A.A., Ang, B.C., Haseeb, A., Wong, Y.C., Wong, Y.H. (2019) Advances in chemiresistive sensors for acetone gas detection. Materials Science in Semiconductor Processing, 103, 104616. https://doi.org/10.1016/j.mssp.2019.104616

Bai, H., Shi, G. (2007) Gas sensors based on conducting polymers. Sensors, 7(3), 267–307.

Bartlett, P.N., Ling-Chung, S.K. (1989) Conducting polymer gas sensors part II: response of polypyrrole to methanol vapour. Sensors and Actuators, 19(2), 141–150. https://doi.org/10.1016/0250-6874(89)87066-0

Bejbouji, H., Vignau, L., Miane, J.L., Dang, M.-T., Oualim, E.M., Harmouchi, M., Mouhsen, A. (2010) Polyaniline as a hole injection layer on organic photovoltaic cells. Solar Energy Materials and Solar Cells, 94(2), 176–181. https://doi.org/10.1016/j.solmat.2009.08.018

Bhardwaj, N., Kundu, S.C. (2010) Electrospinning: a fascinating fiber fabrication technique. Biotechnology Advances, 28(3), 325–347. https://doi.org/10.1016/j.biotechadv.2010.01.004

Bhat, N., Gadre, A., Bambole, V. (2003) Investigation of electropolymerized polypyrrole composite film: Characterization and application to gas sensors. Journal of Applied Polymer Science, 88(1), 22–29. https://doi.org/10.1002/app.11641

Buchko, C.J., Chen, L.C., Shen, Y., Martin, D.C. (1999) Processing and microstructural characterization of porous biocompatible protein polymer thin films. Polymer, 40(26), 7397–7407. https://doi.org/10.1016/S0032-3861(98)00866-0

Cai, Z., Martin, C.R. (1989) Electronically conductive polymer fibers with mesoscopic diameters show enhanced electronic conductivities. Journal of the American Chemical Society, 111(11), 4138–4139. https://doi.org/10.1021/ja00193a077

Casper, C.L., Stephens, J.S., Tassi, N.G., Chase, D.B., Rabolt, J.F. (2004) Controlling surface morphology of electrospun polystyrene fibers: effect of humidity and molecular weight in the electrospinning process. Macromolecules, 37(2), 573–578. https://doi.org/10.1021/ma0351975

Chandler, G., Pletcher, D. (1986) The electrodeposition of metals onto polypyrrole films from aqueous solution. Journal of Applied Electrochemistry, 16(1), 62–68.

Chiang, C., Fincher Jr, C., Park, Y., Heeger, A., Shirakawa, H., Louis, E., Gau, S., MacDiarmid, A.G. (1978) Electrical Conductivity in Doped Polyacetylene. Physical Review Letters, 40(22), 1472. https://doi.org/10.1103/PhysRevLett.39.1098

Chinnappan, A., Baskar, C., Baskar, S., Ratheesh, G., Ramakrishna, S. (2017) An overview of electrospun nanofibers and their application in energy storage, sensors and wearable/flexible electronics. Journal of Materials Chemistry C, 5(48), 12657–12673. https://doi.org/10.1039/C7TC03058D

Choudhary, M., Islam, R.U., Witcomb, M.J., Mallick, K. (2014) In situ generation of a high-performance Pd-polypyrrole composite with multi-functional catalytic properties. Dalton Transactions, 43(17), 6396–6405. https://doi.org/10.1039/C3DT53567C

Chronakis, I.S. (2005) Novel nanocomposites and nanoceramics based on polymer nanofibers using electrospinning process - a review. Journal of Materials Processing Technology, 167(2–3), 283–293. https://doi.org/10.1016/j.jmatprotec.2005.06.053

Das, M., Sarkar, D. (2018) Development of room temperature ethanol sensor from polypyrrole (PPy) embedded in polyvinyl alcohol (PVA) matrix. Polymer Bulletin, 75(7), 3109–3125. https://doi.org/ 10.1007/s00289-017-2192-y

Densakulprasert, N., Wannatong, L., Chotpattananont, D., Hiamtup, P., Sirivat, A., Schwank, J. (2005) Electrical conductivity of polyaniline/zeolite composites and synergetic interaction with CO. Materials Science and Engineering: B, 117(3), 276–282. https://doi.org/10.1016/j.mseb.2004.12.006

Dhand, C., Das, M., Sumana, G., Srivastava, A.K., Pandey, M.K., Kim, C.G., Datta, M., Malhotra, B.D. (2010) Preparation, characterization and application of polyaniline nanospheres to biosensing. Nanoscale, 2(5), 747–754. https://doi.org/10.1039/B9NR00346K

Dixit, V., Misra, S., Sharma, B. (2005) Carbon monoxide sensitivity of vacuum deposited polyaniline semiconducting thin films. Sensors and Actuators B: Chemical, 104(1), 90–93. https://doi.org/10.1016/j.snb.2004.05.001

Dunst, K., Jurków, D., Jasiński, P. (2016) Laser patterned platform with PEDOT-graphene composite film for $NO_2$ sensing. Sensors and Actuators B: Chemical, 229, 155–165. https://doi.org/10.1016/j.snb.2016.01.093

Dunst, K., Karczewski, J., Jasiński, P. (2017) Nitrogen dioxide sensing properties of PEDOT polymer films. Sensors and Actuators B: Chemical, 247, 108–113. https://doi.org/10.1016/j.snb.2017.03.003

Fong, H., Chun, I., Reneker, D.H. (1999) Beaded nanofibers formed during electrospinning. Polymer, 40(16), 4585–4592. https://doi.org/10.1016/S0032-3861(99)00068-3

Formhals, A. (1934) Process and apparatus for preparing artificial threads. US Patent: 1975504, vol, 1, 7.

Fowler, J.D., Virji, S., Kaner, R.B., Weiller, B.H. (2009) Hydrogen detection by polyaniline nanofibers on gold and platinum electrodes. The Journal of Physical Chemistry C, 113(16), 6444–6449. https://doi.org/10.1021/jp810500q

Fratoddi, I., Venditti, I., Cametti, C., Russo, M.V. (2015) Chemiresistive polyaniline-based gas sensors: A mini review. Sensors and Actuators B: Chemical, 220, 534–548. https://doi.org/10.1016/j.snb.2015.05.107

Gardner, J.W., Bartlett, P.N. (2000) Electronic noses. Principles and applications. IOP Publishing.

Geng, L. (2010) Gas sensitivity study of polypyrrole/$WO_3$ hybrid materials to $H_2S$. Synthetic Metals, 160(15–16), 1708–1711. https://doi.org/10.1016/j.synthmet.2010.06.005

Geng, L., Zhao, Y., Huang, X., Wang, S., Zhang, S., Huang, W., Wu, S. (2006) The preparation and gas sensitivity study of polypyrrole/zinc oxide. Synthetic Metals, 156(16), 1078–1082. https://doi.org/10.1016/j.synthmet.2006.06.019

Gerard, M., Chaubey, A., Malhotra, B.D. (2002) Application of conducting polymers to biosensors. Biosensors and Bioelectronics, 17(5), 345–359, https://doi.org/10.1016/S0956-5663(01)00312-8

Gilch, H., Wheelwright, W. (1966) Polymerization of α-halogenated p-xylenes with base. Journal of Polymer Science Part A-1: Polymer Chemistry, 4(6), 1337–1349.

Gu, Z., Ye, J., Song, W., Shen, Q. (2014) Synthesis of polyaniline nanotubes with controlled rectangular or square pore shape. Materials Letters, 121, 12–14. https://doi.org/10.1016/j.matlet.2014.01.133

Guernion, N., Ewen, R., Pihlainen, K., Ratcliffe, N.M., Teare, G. (2002) The fabrication and characterisation of a highly sensitive polypyrrole sensor and its electrical responses to amines of differing basicity at high humidities. Synthetic Metals,

126(2–3), 301–310. https://doi.org/10.1016/S0379-6779(01)00572-0

Haghi, A., Akbari, M. (2007) Trends in electrospinning of natural nanofibers. Physica Status Solidi (a), 204(6), 1830–1834. https://doi.org/10.1002/pssa.200675301

Han, G., Shi, G. (2007) Porous polypyrrole/polymethylmethacrylate composite film prepared by vapor deposition polymerization of pyrrole and its application for ammonia detection. Thin Solid Films, 515(17), 6986–6991. https://doi.org/10.1016/j.tsf.2007.02.007

Hangarter, C.M., Chartuprayoon, N., Hernández, S.C., Choa, Y., Myung, N.V. (2013) Hybridized conducting polymer chemiresistive nano-sensors. Nano Today, 8(1), 39–55. https://doi.org/10.1016/j.nantod.2012.12.005

Hashemi Karouei, S.F., Milani Moghaddam, H. (2019) P-p heterojunction of polymer/hierarchical mesoporous $LaFeO_3$ microsphere as $CO_2$ gas sensing under high humidity. Applied Surface Science, 479, 1029–1038. https://doi.org/10.1016/j.apsusc.2019.02.099

Hayati, I., Bailey, A., Tadros, T.F. (1987) Investigations into the mechanisms of electrohydrodynamic spraying of liquids: I. Effect of electric field and the environment on pendant drops and factors affecting the formation of stable jets and atomization. Journal of Colloid and Interface Science, 117(1), 205–221. https://doi.org/10.1016/0021-9797(87)90185-8

Heeger, A.J. (2001) Semiconducting and metallic polymers: the fourth generation of polymeric materials (Nobel lecture). Angewandte Chemie International Edition, 40(14), 2591–2611. https://doi.org/10.1002/1521-3773(20010716)40:14<2591::AID-ANIE2591>3.0.CO;2-0

Hohman, M.M., Shin, M., Rutledge, G., Brenner, M.P. (2001) Electrospinning and electrically forced jets. II. Applications. Physics of Fluids, 13(8), 2221–2236. https://doi.org/10.1063/1.1384013

Huang, C., Chen, S., Lai, C., Reneker, D.H., Qiu, H., Ye, Y., Hou, H. (2006) Electrospun polymer nanofibres with small diameters. Nanotechnology, 17(6), 1558. https://doi.org/10.1088/0957-4484/17/6/004

Huang, J., Virji, S., Weiller, B.H., Kaner, R.B. (2004) Nanostructured polyaniline sensors. Chemistry - A European Journal, 10(6), 1314–1319. https://doi.org/10.1002/chem.200305211

Huang, Z.-M., Zhang, Y.-Z., Kotaki, M., Ramakrishna, S. (2003) A review on polymer nanofibers by electrospinning and their applications in nanocomposites. Composites Science and Technology, 63(15), 2223–2253. https://doi.org/10.1016/S0266-3538(03)00178-7

Janata, J., Josowicz, M. (2003) Conducting polymers in electronic chemical sensors. Nature Materials, 2(1), 19. https://doi.org/10.1038/nmat768

Jiang, H., Hu, Y., Li, Y., Zhao, P., Zhu, K., Chen, W. (2005a) A facile technique to prepare biodegradable coaxial electrospun nanofibers for controlled release of bioactive agents. Journal of Controlled Release, 108(2–3), 237–243. https://doi.org/10.1016/j.jconrel.2005.08.006

Jiang, L., Jun, H.-K., Hoh, Y.-S., Lim, J.-O., Lee, D.-D., Huh, J.-S. (2005b) Sensing characteristics of polypyrrole-poly (vinyl alcohol) methanol sensors prepared by in situ vapor state polymerization. Sensors and Actuators B: Chemical, 105(2), 132–137. https://doi.org/10.1016/j.snb.2003.12.077

Joshi, A., Gangal, S., Gupta, S. (2011) Ammonia sensing properties of polypyrrole thin films at room temperature. Sensors and Actuators B: Chemical, 156(2), 938–942. https://doi.org/10.1016/j.snb.2011.03.009

Jun, T.-S., Ho, T.A., Rashid, M., Kim, Y.S. (2013) A novel methanol sensor based on gas-penetration through a porous polypyrrole-coated polyacrylonitrile nanofiber mat. Journal of Nanoscience and Nanotechnology, 13(9), 6249–6253. https://doi.org/10.1166/jnn.2013.7693

Jung, S.-H., Kim, H.K., Kim, S.-H., Kim, Y.H., Jeoung, S.C., Kim, D. (2000) Palladium-catalyzed direct synthesis, photophysical properties, and tunable electroluminescence of novel silicon-based alternating copolymers. Macromolecules, 33(25), 9277–9288. https://doi.org/10.1021/ma000 3248

Jung, Y.S., Jung, W., Tuller, H.L., Ross, C. (2008) Nanowire conductive polymer gas sensor patterned using self-assembled block copolymer lithography. Nano Letters, 8(11), 3776–3780. https://doi.org/10.1021/nl802099k

Kayaci, F., Vempati, S., Ozgit-Akgun, C., Biyikli, N., Uyar, T. (2014) Enhanced photocatalytic activity of homoassembled ZnO nanostructures on electrospun polymeric nanofibers: A combination of atomic layer deposition and hydrothermal growth. Applied Catalysis B: Environmental, 156, 173–183. https://doi.org/10.1016/j.apcatb.2014.03.004

Kelly, F.M., Meunier, L., Cochrane, C., Koncar, V. (2013) Polyaniline: Application as solid state electrochromic in a flexible textile display. Displays, 34(1), 1–7. https://doi.org/10.1016/j.displa.2012.10.001

Kim, D.-u., Yoo, B. (2011) A novel electropolymerization method for Ppy nanowire-based $NH_3$ gas sensor with low contact resistance. Sensors and Actuators B: Chemical, 160(1), 1168–1173. https://doi.org/10.1016/j.snb.2011.09.042

Korotcenkov, G. (2007) Metal oxides for solid-state gas sensors: What determines our choice?. Materials Science and Engineering: B, 139(1), 1–23. https://doi.org/10.1016/j.mseb.2007.01.044

Kovtyukhova, N.I., Martin, B., Mbindyo, J., Mallouk, T.E., Cabassi, M., Mayer, T. (2002) Layer-by-layer self-assembly strategy for template synthesis of nanoscale devices. Materials Science and Engineering: C, 19(1–2), 255–262. https://doi.org/10.1016/S0928-4931(01)00395-2

Kriegel, C., Arrechi, A., Kit, K., McClements, D., Weiss, J. (2008) Fabrication, functionalization, and application of electrospun biopolymer nanofibers. Critical Reviews in Food Science and Nutrition, 48(8), 775–797. https://doi.org/10.1080/10408390802241325

Kumar, D., Sharma, R. (1998) Advances in conductive polymers. European Polymer Journal, 34(8), 1053–1060. https://doi.org/10.1016/S0014-3057(97)00204-8

Kumar, E.R., Jayaprakash, R., Devi, G.S., Reddy, P.S.P. (2014) Synthesis of Mn substituted $CuFe_2O_4$ nanoparticles for liquefied petroleum gas sensor applications. Sensors and Actuators B: Chemical, 191, 186–191. https://doi.org/10.1016/j.snb.2013.09.108

Kumar, V., Mahajan, R., Bhatnagar, D., Kaur, I. (2016) Nanofibers synthesis of ND: PANI composite by liquid/liquid interfacial polymerization and study on the effect of NDs on growth mechanism of nanofibers. European Polymer Journal, 83, 1–9. https://doi.org/10.1016/j.eurpolymj.2016.07.025

Kumar, V., Mahajan, R., Kaur, I., Kim, K.-H. (2017) Simple and mediator-free urea sensing based on engineered nanodiamonds with polyaniline nanofibers synthesized in situ. ACS Applied Materials & Interfaces, 9(20), 16813–16823. https://doi.org/10.1021/acsami.7b01948

Le, T.-H., Kim, Y., Yoon, H. (2017) Electrical and electrochemical properties of conducting polymers. Polymers, 9(4), 150. https://doi.org/10.3390/polym9040150

Li, D., Wang, Y., Xia, Y. (2004) Electrospinning nanofibers as uniaxially aligned arrays and layer-by-layer stacked films. Advanced Materials, 16(4), 361–366. https://doi.org/10.1002/adma.200306226

Li, F., Kang, Z., Huang, X., Zhang, G.-J. (2014) Fabrication of zirconium carbide nanofibers by electrospinning. Ceramics International, 40(7), 10137–10141. https://doi.org/10.1016/j.ceramint.2014.02.011

Li, Z., Wang, C. (2013) One-dimensional nanostructures: electrospinning technique and unique nanofibers. Springer.

Lim, C.T. (2017) Nanofiber technology: current status and emerging developments. Progress in Polymer Science, 70, 1–17. https://doi.org/10.1016/j.progpolymsci.2017.03.002

Lin, T., Lv, X., Li, S., Wang, Q. (2017) The morphologies of the semiconductor oxides and their gas-sensing properties. Sensors, 17(12), 2779. https://doi.org/10.3390/s17122779

Lin, Y., Huang, L., Chen, L., Zhang, J., Shen, L., Chen, Q., Shi, W. (2015) Fully gravure-printed $NO_2$ gas sensor on a polyimide foil using $WO_3$-PEDOT:PSS nanocomposites and Ag electrodes. Sensors and Actuators B: Chemical, 216, 176–183. https://doi.org/10.1016/j.snb.2015.04.045

Liu, W., Hu, Y., Hou, Y. (2020) Ethanol Gas Sensitivity Sensor Based on Roughened POF Taper of Modified Polypyrrole Films. Sensors, 20(4), 989. https://doi.org/10.3390/s20040989

Liu, W., Kumar, J., Tripathy, S., Senecal, K.J., Samuelson, L. (1999) Enzymatically synthesized conducting polyaniline. Journal of the American Chemical Society, 121(1), 71–78. https://doi.org/10.1021/ja982270b

Long, Y.-Z., Li, M.-M., Gu, C., Wan, M., Duvail, J.-L., Liu, Z., Fan, Z. (2011) Recent advances in synthesis, physical properties and applications of conducting polymer nanotubes and nanofibers. Progress in Polymer Science, 36(10), 1415–1442. https://doi.org/10.1016/j.progpolymsci.2011.04.001

Mashao, G., Ramohlola, K.E., Mdluli, S.B., Monama, G.R., Hato, M.J., Makgopa, K., Molapo, K.M., Ramoroka, M.E., Iwuoha, E.I., Modibane, K.D. (2019) Zinc-based zeolitic benzimidazolate framework/polyaniline nanocomposite for electrochemical sensing of hydrogen gas. Materials Chemistry and Physics, 230, 287–298. https://doi.org/10.1016/j.matchemphys.2019.03.079

Miasik, J.J., Hooper, A., Tofield, B.C. (1986) Conducting polymer gas sensors. Journal of the Chemical Society, Faraday Transactions 1: Physical Chemistry in Condensed Phases, 82(4), 1117–1126. https://doi.org/10.1039/F19868201117

Miller, D.R., Akbar, S.A., Morris, P.A. (2014) Nanoscale metal oxide-based heterojunctions for gas sensing: a review. Sensors and Actuators B: Chemical, 204, 250–272. https://doi.org/10.1016/j.snb.2014.07.074

Mirzaei, A., Leonardi, S., Neri, G. (2016) Detection of hazardous volatile organic compounds (VOCs) by metal oxide nanostructures-based gas sensors: A review. Ceramics International, 42(14), 15119–15141. https://doi.org/10.1016/j.ceramint.2016.06.145

Mohammadi, A., Hasan, M.-A., Liedberg, B., Lundström, I., Salaneck, W. (1986) Chemical vapour deposition (CVD) of conducting polymers: Polypyrrole. Synthetic Metals, 14(3), 189–197. https://doi.org/10.1016/0379-6779(86)90183-9

Moon, Y.-E., Yun, J., Kim, H.-I. (2013) Synergetic improvement in electromagnetic interference shielding characteristics of polyaniline-coated graphite oxide/$\gamma$-$Fe_2O_3$/$BaTiO_3$ nanocomposites. Journal of Industrial and Engineering Chemistry, 19(2), 493–497. https://doi.org/10.1016/j.jiec.2012.09.002

Neri, G., Donato, N. (1999) Resistive Gas Sensors, Wiley Encyclopedia of Electrical and Electronics Engineering, 1–12.

Nimkar, S.H., Agrawal, S.P., Kondawar, S.B. (2015) Fabrication of electrospun nanofibers of titanium dioxide intercalated polyaniline nanocomposites for $CO_2$ gas sensor. Procedia Materials Science, 10, 572–579. https://doi.org/10.1016/j.mspro.2015.06.008

Nylander, C., Armgarth, M., Lundström, I. (1983) An ammonia detector based on a conducting polymer. Proceedings of the International Meeting on Chemical Sensors, pp. 203–207.

Pandey, S. (2016) Highly sensitive and selective chemiresistor gas/vapor sensors based on polyaniline nanocomposite: a comprehensive review. Journal of Science: Advanced Materials and Devices, 1(4), 431–453. https://doi.org/10.1016/j.jsamd.2016.10.005

Park, S., Park, C., Yoon, H. (2017) Chemo-electrical gas sensors based on conducting polymer hybrids. Polymers, 9(5), 155. https://doi.org/10.3390/polym9050155

Patil, J.V., Mali, S.S., Kamble, A.S., Hong, C.K., Kim, J.H., Patil, P.S. (2017) Electrospinning: A versatile technique for making of 1D growth of nanostructured nanofibers and its applications: An experimental approach. Applied Surface Science, 423, 641–674. https://doi.org/10.1016/j.apsusc.2017.06.116

Patil, P.T., Anwane, R.S., Kondawar, S.B. (2015) Development of electrospun polyaniline/ZnO composite nanofibers for LPG sensing. Procedia Materials Science, 10, 195–204. https://doi.org/10.1016/j.mspro.2015.06.041

Patil, S.L., Chougule, M.A., Sen, S., Patil, V.B. (2012) Measurements on room temperature gas sensing properties of CSA doped polyaniline-ZnO nanocomposites. Measurement, 45(3), 243–249, https://doi.org/10.1016/j.measurement.2011.12.012

Penza, M., Milella, E., Alba, M., Quirini, A., Vasanelli, L. (1997) Selective $NH_3$ gas sensor based on Langmuir-Blodgett polypyrrole film. Sensors and Actuators B: Chemical, 40(2–3), 205–209. https://doi.org/10.1016/S0925-4005(97)80263-

8
Pillay, V., Dott, C., Choonara, Y.E., Tyagi, C., Tomar, L., Kumar, P., du Toit, L.C., Ndesendo, V.M. (2013) A review of the effect of processing variables on the fabrication of electrospun nanofibers for drug delivery applications. Journal of Nanomaterials, 2013. https://doi.org/10.1155/2013/789289
Pinto, N.J., Rivera, D., Melendez, A., Ramos, I., Lim, J.H., Johnson, A.C. (2011) Electrical response of electrospun PEDOT-PSSA nanofibers to organic and inorganic gases. Sensors and Actuators B: Chemical, 156(2), 849–853. https://doi.org/10.1016/j.snb.2011.02.053
Rahy, A., Yang, D.J. (2008) Synthesis of highly conductive polyaniline nanofibers. Materials Letters, 62(28), 4311–4314. https://doi.org/10.1016/j.matlet.2008.06.057
Ramakrishna, S., Fujihara, K., Teo, W.-E., Yong, T., Ma, Z., Ramaseshan, R. (2006) Electrospun nanofibers: solving global issues. Materials Today, 9(3), 40–50, https://doi.org/10.1016/S1369-7021(06)71389-X
Rojas, R., Pinto, N.J. (2008) Using electrospinning for the fabrication of rapid response gas sensors based on conducting polymer nanowires. IEEE Sensors Journal, 8(6), 951–953. https://doi.org/10.1109/JSEN.2008.923932
Sadek, A.Z., Wlodarski, W., Kalantar-Zadeh, K., Baker, C., Kaner, R.B. (2007) Doped and dedoped polyaniline nanofiber based conductometric hydrogen gas sensors. Sensors and Actuators A: Physical, 139(1), 53–57. https://doi.org/10.1016/j.sna.2006.11.033
Samui, A., Patankar, A., Satpute, R., Deb, P. (2001) Synthesis and characterization of polyaniline-maleic acid salt. Synthetic Metals, 125(3), 423–427. https://doi.org/10.1016/S0379-6779(01)00487-8
Seiyama, T., Kato, A., Fujiishi, K., Nagatani, M. (1962) A new detector for gaseous components using semiconductive thin films. Analytical Chemistry, 34(11), 1502–1503. https://doi.org/10.1021/ac60191a001
Sen, T., Mishra, S., Shimpi, N.G. (2016) Synthesis and sensing applications of polyaniline nanocomposites: a review. RSC Advances, 6(48), 42196–42222. https://doi.org/10.1039/C6RA03049A
Sharma, H.J., Sonwane, N.D., Kondawar, S.B. (2015) Electrospun $SnO_2$/Polyaniline composite nanofibers based low temperature hydrogen gas sensor. Fibers and Polymers, 16(7), 1527–1532. https://doi.org/10.1007/s12221-015-5222-0
Shimizu, Y., Egashira, M. (1999) Basic aspects and challenges of semiconductor gas sensors. Mrs Bulletin, 24(6), 18–24. https://doi.org/10.1557/S0883769400052465
Shirakawa, H., Louis, E.J., MacDiarmid, A.G., Chiang, C.K., Heeger, A.J. (1977) Synthesis of electrically conducting organic polymers: halogen derivatives of polyacetylene, (CH)x. Journal of the Chemical Society, Chemical Communications(16), 578–580. https://doi.org/10.1039/C39770000578
Shirsat, M.D., Bangar, M.A., Deshusses, M.A., Myung, N.V., Mulchandani, A. (2009) Polyaniline nanowires-gold nanoparticles hybrid network based chemiresistive hydrogen sulfide sensor. Applied Physics Letters, 94(8), 083502. https://doi.org/10.1063/1.3070237
Skotheim, T.A., Reynolds, J. (2007) Handbook of conducting polymers, 2 volume set. CRC press.
Song, X., Xu, Q., Xu, H., Cao, B. (2017) Highly sensitive gold-decorated zinc oxide nanorods sensor for triethylamine working at near room temperature. Journal of Colloid and Interface Science, 499, 67–75. https://doi.org/10.1016/j.jcis.2017.03.092
Sowmiya, T., Ananthi, A., Anandhakumar, S., Mathiyarasu, J. (2012) Potentiometric glucose biosensing using camphor sulfonic acid doped polyaniline. Analytical Methods, 4(6), 1838–1842. https://doi.org/10.1039/C2AY25215E
Starr, J.D., Andrew, J.S. (2013) A route to synthesize multifunctional tri-phasic nanofibers. Journal of Materials Chemistry C, 1(14), 2529–2533. https://doi.org/10.1039/C3TC00949A
Stejskal, J., Omastova, M., Fedorova, S., Prokeš, J., Trchová, M. (2003) Polyaniline and polypyrrole prepared in the presence of surfactants: a comparative conductivity study. Polymer, 44(5), 1353–1358. https://doi.org/10.1016/S0032-3861(02)00906-0
Su, P.-G., Liao, S.-L. (2016) Fabrication of a flexible $H_2$ sensor based on Pd nanoparticles modified polypyrrole films. Materials Chemistry and Physics, 170, 180–185. https://doi.org/10.1016/j.matchemphys.2015.12.037
Su, P.-G., Shiu, C.-C. (2011) Flexible $H_2$ sensor fabricated by layer-by-layer self-assembly of thin films of polypyrrole and modified in situ with Pt nanoparticles. Sensors and Actuators B: Chemical, 157(1), 275–281. https://doi.org/10.1016/j.snb.2011.03.062
Subbiah, T., Bhat, G.S., Tock, R.W., Parameswaran, S., Ramkumar, S.S. (2005) Electrospinning of nanofibers. Journal of Applied Polymer Science, 96(2), 557–569. https://doi.org/10.1002/app.21481
Sukigara, S., Gandhi, M., Ayutsede, J., Micklus, M., Ko, F. (2003) Regeneration of Bombyx mori silk by electrospinning - part 1: processing parameters and geometric properties, Polymer, 44(19), 5721–5727. https://doi.org/10.1016/S0032-3861(03)00532-9
Sun, J., Shu, X., Tian, Y., Tong, Z., Bai, S., Luo, R., Li, D., Chen, A. (2017) Preparation of polypyrrole@ $WO_3$ hybrids with pn heterojunction and sensing performance to triethylamine at room temperature. Sensors and Actuators B: Chemical, 238, 510–517. https://doi.org/10.1016/j.snb.2016.07.012
Sun, Z., Zussman, E., Yarin, A.L., Wendorff, J.H., Greiner, A. (2003) Compound core-shell polymer nanofibers by co-electrospinning. Advanced Materials, 15(22), 1929–1932. https://doi.org/10.1002/adma.200305136
Sundaray, B., Subramanian, V., Natarajan, T., Xiang, R.-Z., Chang, C.-C., Fann, W.-S. (2004) Electrospinning of continuous aligned polymer fibers. Applied Physics Letters, 84(7), 1222–1224. https://doi.org/10.1063/1.1647685
Taguchi, N. (1962) A metal oxide gas sensor, Japanese patent, 4538200.
Talwar, V., Singh, O., Singh, R.C. (2014) ZnO assisted polyaniline nanofibers and its application as ammonia gas sensor. Sensors and Actuators B: Chemical, 191, 276–282. https://doi.org/10.1016/j.snb.2013.09.106
Tan, S.-H., Inai, R., Kotaki, M., Ramakrishna, S. (2005) Systematic parameter study for ultra-fine fiber fabrication via elec-

trospinning process. Polymer, 46(16), 6128–6134. https://doi.org/10.1016/j.polymer.2005.05.068

Tandon, R., Tripathy, M., Arora, A., Hotchandani, S. (2006) Gas and humidity response of iron oxide-polypyrrole nanocomposites. Sensors and Actuators B: Chemical, 114(2), 768–773. https://doi.org/10.1016/j.snb.2005.07.022

Teo, W.E., Ramakrishna, S. (2006) A review on electrospinning design and nanofibre assemblies. Nanotechnology, 17(14), R89. https://doi.org/10.1088/0957-4484/17/14/R01

Thenmozhi, S., Dharmaraj, N., Kadirvelu, K., Kim, H.Y. (2017) Electrospun nanofibers: New generation materials for advanced applications. Materials Science and Engineering: B, 217, 36–48. https://doi.org/10.1016/j.mseb.2017.01.001

Tomaszewski, W., Szadkowski, M. (2005) Investigation of electrospinning with the use of a multi-jet electrospinning head. Fibres and Textiles in Eastern Europe, 13(4), 22–26.

Tran, C., Kalra, V. (2013) Co-continuous nanoscale assembly of Nafion-polyacrylonitrile blends within nanofibers: a facile route to fabrication of porous nanofibers. Soft Matter, 9(3), 846–852. https://doi.org/10.1039/C2SM25976A

Virji, S., Kaner, R.B., Weiller, B.H. (2006) Hydrogen sensors based on conductivity changes in polyaniline nanofibers. The Journal of Physical Chemistry B, 110(44), 22266–22270. https://doi.org/10.1021/jp063166g

Wang, C., Yin, L., Zhang, L., Xiang, D., Gao, R. (2010) Metal oxide gas sensors: sensitivity and influencing factors. Sensors, 10(3), 2088–2106. https://doi.org/10.3390/s100302088

Wang, X., Niu, H., Lin, T., Wang, X. (2009a) Needleless electrospinning of nanofibers with a conical wire coil. Polymer Engineering & Science, 49(8), 1582–1586. https://doi.org/10.1002/pen.21377

Wang, X., Sun, K., Li, K., Li, X., Gogotsi, Y. (2019) $Ti_3C_2T_x$/PEDOT:PSS hybrid materials for room-temperature methanol sensor. Chinese Chemical Letters, https://doi.org/10.1016/j.cclet.2019.11.031

Wang, X., Um, I.C., Fang, D., Okamoto, A., Hsiao, B.S., Chu, B. (2005) Formation of water-resistant hyaluronic acid nanofibers by blowing-assisted electro-spinning and non-toxic post treatments. Polymer, 46(13), 4853–4867. https://doi.org/10.1016/j.polymer.2005.03.058

Wang, Y., Jia, W., Strout, T., Schempf, A., Zhang, H., Li, B., Cui, J., Lei, Y. (2009b) Ammonia Gas Sensor Using Polypyrrole-Coated $TiO_2$/ZnO Nanofibers. Electroanalysis: An International Journal Devoted to Fundamental and Practical Aspects of Electroanalysis, 21(12), 1432–1438. https://doi.org/10.1002/elan.200904584

Wetchakun, K., Samerjai, T., Tamaekong, N., Liewhiran, C., Siriwong, C., Kruefu, V., Wisitsoraat, A., Tuantranont, A., Phanichphant, S. (2011) Semiconducting metal oxides as sensors for environmentally hazardous gases, Sensors and Actuators B: Chemical, 160(1), 580–591. https://doi.org/10.1016/j.snb.2011.08.032

Wong, S.-C., Baji, A., Leng, S. (2008) Effect of fiber diameter on tensile properties of electrospun poly (ε-caprolactone). Polymer, 49(21), 4713–4722. https://doi.org/10.1016/j.polymer.2008.08.022

Wong, Y.C., Ang, B.C., Haseeb, A., Baharuddin, A.A., Wong, Y.H. (2019) Conducting Polymers as Chemiresistive Gas Sensing Materials: A Review. Journal of The Electrochemical Society, 167(3), 037503. https://doi.org/10.1149/2.0032003JES

Xie, Y., Du, J., Zhao, R., Wang, H., Yao, H. (2013) Facile synthesis of hexagonal brick-shaped $SnO_2$ and its gas sensing toward triethylamine. Journal of Environmental Chemical Engineering, 1(4), 1380–1384. https://doi.org/10.1016/j.jece.2013.08.021

Xu, C., Inai, R., Kotaki, M., Ramakrishna, S. (2004) Aligned biodegradable nanofibrous structure: a potential scaffold for blood vessel engineering. Biomaterials, 25(5), 877–886. https://doi.org/10.1016/s0142-9612(03)00593-3

Yamazoe, N. (1991) New approaches for improving semiconductor gas sensors. Sensors and Actuators B: Chemical, 5(1–4), 7–19. https://doi.org/10.1016/0925-4005(91)80213-4

Yamazoe, N. (2005) Toward innovations of gas sensor technology. Sensors and Actuators B: Chemical, 108(1–2), 2–14. https://doi.org/10.1016/j.snb.2004.12.075

Yang, X., Yu, Q., Zhang, S., Sun, P., Lu, H., Yan, X., Liu, F., Zhou, X., Liang, X., Gao, Y. (2018) Highly sensitive and selective triethylamine gas sensor based on porous $SnO_2$/$Zn_2SnO_4$ composites. Sensors and Actuators B: Chemical, 266, 213–220. https://doi.org/10.1016/j.snb.2018.03.044

Yang, Z., Hu, B., Karasz, F. (1995) Polymer electroluminescence using ac or reverse dc biasing. Macromolecules, 28(18), 6151–6154. https://doi.org/10.1021/ma00122a023

Yanılmaz, M., Sarac, A.S. (2014) A review: effect of conductive polymers on the conductivities of electrospun mats. Textile Research Journal, 84(12), 1325–1342. https://doi.org/10.1177/0040517513495943

Yoon, H., Chang, M., Jang, J. (2006) Sensing behaviors of polypyrrole nanotubes prepared in reverse microemulsions: effects of transducer size and transduction mechanism. The Journal of Physical Chemistry B, 110(29), 14074–14077. https://doi.org/10.1021/jp061423b

Zampetti, E., Pantalei, S., Muzyczuk, A., Bearzotti, A., De Cesare, F., Spinella, C., Macagnano, A. (2013) A high sensitive $NO_2$ gas sensor based on PEDOT-PSS/$TiO_2$ nanofibres. Sensors and Actuators B: Chemical, 176, 390–398. https://doi.org/10.1016/j.snb.2012.10.005

Zhang, Y., Huang, Z.-M., Xu, X., Lim, C.T., Ramakrishna, S. (2004) Preparation of core-shell structured PCL-r-gelatin bi-component nanofibers by coaxial electrospinning. Chemistry of Materials, 16(18), 3406–3409. https://doi.org/10.1021/cm049580f

Zhao, X., Kim, J.-K., Ahn, H.-J., Cho, K.-K., Ahn, J.-H. (2013) A ternary sulfur/polyaniline/carbon composite as cathode material for lithium sulfur batteries. Electrochimica Acta, 109, 145–152. https://doi.org/10.1016/j.electacta.2013.07.067

Zou, Y., Wang, Q., Xiang, C., Tang, C., Chu, H., Qiu, S., Yan, E., Xu, F., Sun, L. (2016) Doping composite of polyaniline and reduced graphene oxide with palladium nanoparticles for room-temperature hydrogen-gas sensing. International Journal of Hydrogen Energy, 41(11), 5396–5404. https://doi.org/10.1016/j.ijhydene.2016.02.023